SOK: Side Channel Monitoring for Additive Manufacturing - Bridging Cybersecurity and Quality Assurance Communities

Muhammad Ahsan, Muhammad Haris Rais, Irfan Ahmed
Department of Computer Science
Virginia Commonwealth University, Richmond, USA
Email: {ahsanm5, raismh, iahmed3}@vcu.edu

Abstract—Additive Manufacturing (AM) is critical for the fourth industrial revolution (i.e., Industry 4.0). It involves printing a 3D object layer-by-layer from scratch. Fused filament fabrication (FFF), one of the most widely used AM technology, has been adopted by commercial and domestic consumers. With the recent addition of metal filaments, FFF caters to a broad spectrum of manufacturing industry requirements. Cybersecurity and Quality Assurance (QA) of the FFF process is an active research area. Like any other cyber-physical system, FFF exhibits many side channels (SCs), including acoustic and thermal emissions, vibrations, etc. Researchers in the QA domain use SCs to predict defects in the printed parts. Cybersecurity researchers, on the other hand, utilize SCs to identify malicious anomalies in the process. While the aims are different, there are definite overlaps in both communities' acquisition and analysis methodologies. As the two communities bring distinct skill sets and expertise, we find an opportunity to bring them closer through a systematic study of available work and identifying the commonalities and distinctions to motivate the consumption of cross-domain knowledge. Our approach to systematizing the knowledge is based on identifying the available SC, the acquisition and analysis methodologies, performance statistics, associated challenges, and future research directions. This knowledge consolidation and systematization exercise will not only help the new researchers aiming to explore SCs in the FFF process but also highlight collaboration opportunities between QA and cybersecurity communities.

Index Terms—Additive Manufacturing, Side Channels, Sabotage, Defense

1. Introduction

With the changing industry verticals and adoption of smart manufacturing, the use of additive manufacturing (AM) is increasing, with its projected growth estimated at $44.6 billion by 2028 [1]. AM, commonly referred to as 3D printing, is the process of creating a physical object from a 3D model. AM enables manufacturers to produce complex geometries with granular control compared to traditional subtractive manufacturing.

From its introduction back in 1987 [2], AM, with its limited usage and high cost, has gone through many advancements to the point where even a home user can purchase a small-scale 3D printer. These days, AM is used in the aerospace industry to design, and prototype rocket parts [3], UAV (unmanned aerial vehicle) components,

the medical sector for developing prosthetic implants, transportation, etc. GE aviation [4] used AM to build the world's first passenger jet engine with a 3D-printed fuel nozzle. The engines are expected to be lighter with 5x more durability and are 20% more heat resilient than traditional engines.

Fused Filament Fabrication (FFF) is rapidly growing and vastly adopted AM technology and is one of the seven AM classes broadly categorized by the American society for testing and materials (ASTM) [3]. FFF is a material extrusion-based AM process that includes extruding a heated filament through a nozzle and depositing layer by layer to create a 3D object. Because of its rapid adoption in commercial and consumer settings, AM is getting in the spotlight of adversaries and becoming a potential target.

3D printers are a cyber-physical system (CPS) that leaks process information in the physical domain. The measurement and analysis of this physical domain data termed side channel (SC) could potentially reveal information that could help detect process anomalies. Cybersecurity researchers have used SCs for in-situ and real-time monitoring of the FFF process to detect cyberattacks on a printed object or a printing environment.

Similarly, QA researchers explore SCs to identify defects in printed objects accurately. While the FFF process allows for the fabrication of more complex geometries and saves time and material wastage, it needs to achieve precision and quality in a final 3D print. According to a study, [5], the failure rate in the FFF process could reach up to 20%. These numbers are majorly attributed to incorrect parameters controlling the printing process and sensitivity to environmental conditions. Therefore, monitoring these controlled and uncontrolled parameters is critical for QA in the FFF process.

While both cybersecurity and QA research communities have a different process-monitoring focus, there are definite overlaps in the SC monitoring techniques used by both communities. This paper presents a systematic study of available literature about SCs use in QA and cybersecurity. Overall, the accuracy and precision of an SC are vital for designing a monitoring scheme. Our analysis reveals that using multiple sensors is more precise for detecting process anomalies. Similarly, power signals provide more accurate results but are limited to kinetic-type anomalies. Several factors, such as sensor intrusiveness, precision, noise, and printing-environment variables, should be considered while designing a monitoring technique.

Key contributions of this study are as follows:

- Consolidation of knowledge related to the use of SCs in QA and cybersecurity for detecting process anomalies in FFF-based AM process.
- A systematization methodology based on identifying the available SCs, and the acquisition and analysis methodologies.
- Performance evaluation of existing SCs to identify research gaps.
- Providing in-depth insights through establishing an association between SCs and printing parameters with process anomalies.
- Identification of commonalities and distinctions between QA and cybersecurity domains to consume cross-domain knowledge and emphasize collaboration opportunities.

The rest of the paper is organized as follows. Section 2 presents motivation and required background, followed by methodology and systematization approach in Section 3. Section 5 presents the categorization of process anomalies. Systematization of existing research efforts is presented in Section 6. Section 7 discusses accuracy and challenges associated with each SC, followed by recommendations and future directions. Section 8 concludes the paper.

2. Motivation and Background

This section details the motivation for the current study, followed by a brief background of the FFF process chain.

2.1. Motivation

Available taxonomies and surveys in QA and cybersecurity domain for monitoring the FFF process using SCs, don't identify and relate the commonalities between the two communities. Fu et al. [6] presented a literature review for in-situ monitoring techniques for the FFF process focusing on the QA aspect of it. Similarly, Yampolskiy et al. [7] presented a comprehensive attack taxonomy and survey for AM but didn't relate QA to it. Another attack taxonomy as presented by Ahmad et al. [8] accounts for the attacker's perspective and motives to understand the relationship between quality control (QC) and CPS attacks in the manufacturing process. The study, however, is limited to threat identification, and the later stages, i.e., detection and response, were not integrated. Therefore, a need to link these studies and consolidate the extensive work in the domain of QC and CPS security is inevitable to reap the best of both domains.

Attacks in FFF can be majorly categorized as IP theft, sabotage, and illegal part manufacturing [7]. In sabotage attacks, the adversary targets the product or printing process with the aim to reduce its mechanical strength, change the part design or impart damage to the equipment. SC in the security domain is being used to detect such anomalies whilst in QA SC is used to validate print integrity and detect defective print. Key quality characteristics are used to ensure that the product remains in conformance with the design intent in terms of geometry, mechanical properties, etc. Regardless of monitoring terminologies or the technique used, the goal

of both domains is to monitor and prevent any anomalies or defects in the printing process/print.

Adding QC perspective to it, the process-anomaly (or anomaly) can therefore be defined as any malicious or uncontrollable action that deters the product quality or printer's performance leading to non-conformance of the user's design intent.

2.2. FFF Process Chain

The FFF process starts by creating a 3D object design in computer-aided design (CAD) software. The design file is typically converted to standard triangle language (STL) format comprising the object's outer geometry information as a set of adjoining triangles. The STL file is then transferred to a slicing software that converts it into printer-specific instructions (called G-codes) using selected printing parameters such as layer thickness, internal structure, and temperature profile. G-codes are sent to the printer via USB or network interface where the printer firmware interprets and sequentially executes these instructions layer after layer to print the object.

3. Systematization Approach

Figure 1 represents the systematization approach used in the presented study. Five components are used to systematize the current knowledge base; i) printing process parameters, ii) process-anomalies targets, iii) side channels, iv) master profile requirement, and v) the research methodology. The proposed systematization approach uses side channel (**SC**) to monitor process anomalies (**A**) that could be the effect of inconsistent printing parameters (**P**). Methodology (**M**) is used to provide correlation between the physical domain data, obtained through side channels (**SCs**) and the process-anomaly (**A**). The study shows that the proposed approach effectively and usefully summarizes relevant literature from the QA and cybersecurity domains using the mentioned five components.

For example, Brion et al. [9] use computer vision to detect warping defects in the print object. Labeled images were used to train a deep convolution neural network (CNN) to predict warpage in real time. In this case in point, the side channel (SC) is 'Optical', monitored process anomaly (A) is 'Warpage' and the methodology (M) used is 'machine learning and image processing'. The components used in the systematization approach are detailed below.

Side Channels (SCs): These refer to the physical domain data that is being exploited/used for detecting/monitoring process-anomaly. A total of eight SCs were selected in this study based on quantitative and qualitative research available in the literature. These include acoustic (SC_A), electric current (SC_I), thermal (SC_T), optical (SC_O), laser (SC_L), pressure (SC_P), vibration (SC_V), and heterogeneous sensors (SC_H).

Parameters (P): These are the variables that are set/controlled, before/during the printing process. Any anomalous alterations to them could potentially change the part properties. A selected set of printing parameters based on their potential effect on the printed object, significance for contributing to complying with the design intent, and use by the community to impart defect were chosen and
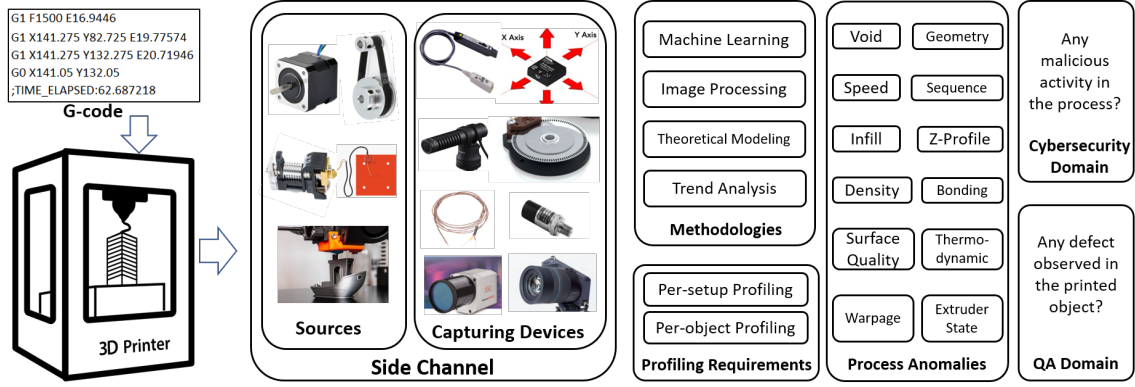
Figure 1. Systematization approach for Side Channels in FFF process

are detailed in Table 1. Material counterpart (P_m) in Table 1 has been added for completeness, but since it is not much explored using SC monitoring, therefore, is not further detailed in systematization.

Process Anomalies (A): These are the potential anomalies/defects that are being monitored using SCs and are further detailed in section 5.

Methodology (M): These are state-of-the-art techniques that are being employed by researchers, for detecting process anomalies through the data obtained using different SC. We have defined four categories to relate the literature to these methodologies.

- Machine Learning **(M1)**: The data collected from different side channels **(SCs)** trains machine learning (ML) models to predict process anomaly **(A)**.
- Image Processing **(M2)**: The digital image is processed using different algorithms to collect information used for later analysis.
- Mathematical/Statistical approach **(M3)**: Theoretical modeling of a process is done and the findings are used for comparative analysis against the results obtained from experimental studies.
- Trend/Data Analysis/Comparison **(M4)**: The experimental data is evaluated either by plotting and analyzing the trends or by comparing it against some set thresholds.

Profiling Requirements: Based on the need for a master profile the current research efforts could be divided into two categories. The first category makes up for those efforts that need a per-object profile to compare and look for anomalies in the print object. These profiles could be a CAD model from a design file or rendered G-code data, or an ideal print object. The second includes those that don't require such profile or source of truth to make predictions instead can either be trained on features extracted from an anomaly or using the correlation of the ground truth sensor data with previous data trends to make future predictions.

For example, in image processing, one might need a source profile to compare and detect process anomalies. For each print geometry, the source profile would be different. On the other hand, if a technique is trained using offline data of a process anomaly and is not limited to a particular geometry, then the predictions are made using the trained algorithm without requiring per-object profiles.

TABLE 1. LIST OF PRINTING PARAMETERS

Parameter Name	Symbol	Definition
Infill Density	P_{id}	Density of the internal supporting structure measured in percentage.
Infill Pattern	P_{ip}	Defines the way the internal structure is arranged. There can be many arrangements including honeycomb, line, rectilinear etc.
Raster Angle	P_{ir}	Angle between the specimen principle axis and the build platform x-axis.
Nozzle Temperature	P_{nt}	Temperature of the print head nozzle needed to melt material for extrusion.
Extruder Feedrate	P_{ef}	Measured in mm/s, defines the speed at which the filament is being extruded from the nozzle and is governed by the extruder motor (e-axis) of printer.
Layer Thickness	P_{lt}	z-axis defines the layer thickness in the print geometry.
Bed Temperature	P_{bt}	Temperature of the print bed needed to attain proper inter/first-layer bonding.
Nozzle Speed	P_{ns}	Also termed as printing speed measured in mm/s normalize the cooling time needed for proper interlayer bonding and reduced thermal stresses.
Axis	P_{ax}	The x,y-axis motors engage the print head and define the print geometry in these two dimensions.
Material	P_m	Material type effectively changes the chemical and mechanical properties of the print.
Fan Speed	P_{fs}	The fan in the printing process provides the cooling effect needed to stabilize the fused filament and the print geometry.

4. FFF Security/QA Goals

In order to better understand security objectives for a FFF process, we first need to perceive the attacker's intent. The goal of an adversary is to either steal intellectual property (IP) or manipulate the printing process to render the printed object useless/defective. Researchers have demonstrated multiple obvious and concealed, high and low magnitude attacks on the printing process to decrease the fatigue life of print by introducing defects in the object [10]–[12]. As the attacks target the physical side of the cyber-physical chain, conventional cybersecurity methods do not offer optimal solutions. Being a cyber-physical system, AM offers additional information sources (side channels) that cybersecurity researchers are leveraging to detect malicious intrusions in the printing process.

The goal of quality assurance is to ensure that the entire process chain is optimized to achieve a final printed object that complies with the design specifications. QA scope also covers the issues raised due to machine hardware problems. A monitoring scheme should therefore maintain and optimize the printing parameters and machine state to guarantee a reliable and defect-free product.

Ref.	Side Channel	Printer	Method -ology	Acc.	Err.
[15]	SC_A	Printrbot	M1	78.35%	17.82%
[16]		Printrbot	M1	86%	11.11%
[13]	SC_I	Lulzbot Taz 6	M4	99%	0.79%
[17]	SC_T	Printrbot	M1, M2	–	–
[18]	SC_O	Rostock Max	M1	–	$0.71mm$
[19]	SC_H	Printrbot	M1	78.35%	17.82%
[21]		Printrbot	M4	–	–
[20]		Lulzbot Taz 5	M1	–	$1mm$
[14]		Ultimaker 2	M1	93.55%	5.87%

4.1. IP Theft

Information Property (IP) theft poses a serious threat to additive manufacturing because manufacturers rely on producing designs that are better, cheaper, and easier to adopt than their competitors. Leaking such information can jeopardize their market standing. An end-to-end secure AM system is still susceptible to IP leaks because of the emanations generated from the printing equipment. Adversaries can use this side-channel information to gain insights into the printing process, such as the material used, feed rate, and part geometry. Therefore, to fully unlock the potential of AM technology, it is crucial to understand and mitigate such threats.

Table 2 lists literature related to IP theft. The table includes the types of SCs that researchers have used to get IP information, as well as the achieved accuracy and errors in prediction. It can be noted that current (SC_I) achieves the maximum accuracy of 99% [13] in estimating the object geometry followed by the heterogeneous sensor (SC_H) with 93.55% [14]. Researchers have mostly employed ML techniques to train and predict print geometry [14]–[20]. ML technique is restricted to per setup basis wherein prediction accuracy is greatly affected by the printer and the sensors used. Therefore, in addition, researchers have also added post/pre-processing manual steps to improve prediction accuracy [20].

4.2. Sabotage

The process anomalies if intentional aims at deterring the part quality such that making it rendered useless or fail during operation. Researchers have proposed to use SCs to detect any adversarial attempt to sabotage the process or add a vulnerability particular to print dynamics. Table 3 lists studies related to sabotage anomalies with the corresponding compromised elements, sabotage stealthiness, and the printing parameters that are being manipulated to compromise the printed object. To sabotage the printing process, an attacker could add adversarial changes to the 3D design file, G-code instructions, slicing parameters, and/or firmware of the printing equipment and thus act as a compromise element for them to add process anomalies.

On the level of visual deformation and stealthiness in the print object, an anomaly could be categorized into Low ○, Medium ◖ and High ● stealth attacks. Where, Low ○ stealthiness attacks can easily be detected through visual inspection. Medium ◖ on the other hand, don't have visual deformation in the finished geometry, but can easily be detected by low-precision detection schemes or manual inspection during the printing process. High ● stealth attacks are smart and concealed in the finished
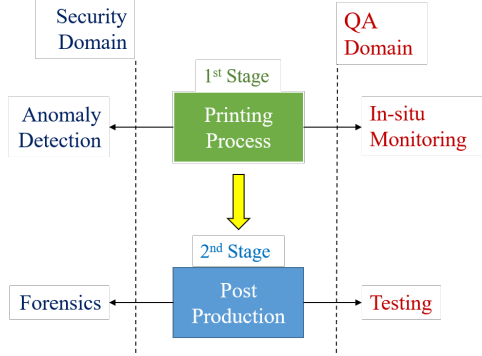

Figure 2. Stages of FFF Process Monitoring

geometry. These are hard to detect and could only be identified using high-precision post-production/in-situ inspection/monitoring techniques.

A void, for example, if visible in the final print object categorized as low, if obfuscated in the finished print but could be easily detected using in-situ monitoring or manual in-process inspection termed as medium, but if it requires high precision monitoring techniques to be detected it is categorized as high stealth anomaly.

4.3. Quality Assurance

To ensure a reliable and defect-free manufactured product, QA is an essential component in AM production chain. Factors like nozzle clogging, material runout, under/over-filling, etc. lead to defects in the manufactured 3D product. A reliable monitoring system should therefore be able to foresee such conditions and stop printing in case of a failure state, as stopping helps reduce material wastage and more importantly saves production time.

QA in the FFF process as shown in Figure 2, can be done in two stages, print monitoring also termed in-situ process monitoring, and post-production testing. The first as the name suggests is done while the machine is in a printing state. There are many factors that can affect the efficient working of the FFF process; those could be internal like erroneous printing parameters or could be external hardware defects like material runout, nozzle clogging, etc. Post-production testing (forensics & testing) [46] on the other hand is done once the printing process has ended and a finished 3D geometry is available.

In-situ process monitoring is done using SCs and could be non-intrusive such as measuring acoustic emanations, or the vibrations produced during the printing process, or it could be intrusive e.g. using an encoder attached to the printer to measure extruder speed. These channels can help give information about the state of the printer itself and the quality of the built object. Different states of the printing machine and the detected printing defects are studied in the literature. Quality is maintained by monitoring characteristic properties, also referred to as Key Quality Characteristics of the print object.

5. Process Anomalies

As defined earlier process anomalies can either be sabotage attacks or defects due to incorrect printing parameters. These anomalies serve as a target for monitoring schemes. Anomalies can be categorized into 3

TABLE 3. EXISTING STUDIES ON SABOTAGE ATTACKS AND THEIR STEALTHINESS

| Ref. | Compromised Element | Stealth | Process Anomaly | Affected Printing Parameters (P) | | | | | | | | | | |
| | | | | P_{if} | | | P_{nt} | P_{ef} | P_{lt} | P_{bt} | P_{ns} | P_{ax} | P_{m} | P_{fs} |
				P_{id}	P_{ip}	P_{ir}								
[22]	Firmware	○	A_{fd},A_{gm}					✓						
[23]	Firmware	◐	A_{fd}					✓						
[24]	GCODE, Slicing parameters	●	$A_{vd},A_{fd},A_{ps},$ $A_{tm},A_{if},A_{zp},A_{gm}$	✓	✓	✓		✓	✓		✓	✓		
[25]	GCODE, Slicing parameters	●	A_{fd},A_{ps},A_{tm}					✓			✓			
[10]	Design file	●	A_{vd}											
[26]	GCODE	◐	A_{vd}								✓	✓		
[27]	Firmware	◐	A_{fd},A_{ps}					✓			✓	✓		
[28]	GCODE	●	A_{vd},A_{ps},A_{tm}								✓	✓		
[29]	Design file	●	A_{if}	✓	✓									
[30]	Design file	◐	A_{if}	✓	✓									
[31]	N/A	◐	A_{if}	✓	✓									
[32], [33]	Design file, Slicing parameters	◐	A_{vd},A_{if}			✓								
[34]	Design file, GCODE	◐	A_{vd},A_{zp}						✓					
[35]	Design file, GCODE	◐	A_{vd},A_{zp}						✓					
[36]	Firmware	◐	$A_{ps},A_{if},A_{th},A_{zp}$	✓					✓		✓		✓	
[11]	GCODE	●	A_{vd},A_{fd},A_{th}				✓	✓						
[37]	GCODE	●	A_{vd}											
[38]	GCODE, Slicing parameters	●	$A_{vd},A_{fd},A_{ps},A_{tm},$ $A_{if},A_{th},A_{zp},A_{gm}$	✓	✓	✓	✓	✓	✓	✓	✓	✓		
[39]	GCODE, Firmware	●	$A_{vd},A_{fd},A_{if},$ A_{zp},A_{gm}		✓				✓		✓	✓		
[40]	Slicing parameters	●	A_{vd},A_{if}				✓							
[12]	Firmware	◐	A_{th}				✓			✓				
[41]	N/A	◐	A_{if}	✓										
[42]–[44]	N/A	◐	A_{gm}										✓	
[45]	N/A	◐	A_{th}											✓

TABLE 4. PROCESS ANOMALIES AND THEIR AFFECTED DOMAINS

Symbol	Process Anomalies	Affected Domain
A_{vd}	Voids	FK, NK, TH
A_{fd}	Filament Density	FK
A_{ps}	Print Speed	NK
A_{tm}	Toolpath Manipulation	FK, NK, TH
A_{if}	Infill Anomaly	FK, NK
A_{th}	Thermodynamics	TH
A_{zp}	Z-Profile	ZK
A_{gm}	Geometry	ZK, FK, NK, TH
A_{sq}	Surface Quality	FK, NK, TH
A_{w}	Warpage	TH
A_{b}	Bonding	ZK, FK, NK, TH
A_{es}	Extruder State	FK, NK, TH

major types: kinetic, thermodynamic, and hybrid as shown in Figure 3. The first type is related to the kinetic properties of the printing process and includes Filament Kinetics (FK), Nozzle Kinetics (NK), and Z-profile (ZK) type anomalies. Thermodynamics (TH) defines the temperature-related print anomalies including nozzle temperature, bed temperature, and fan speed process variations. Hybrid, on the other hand, amounts to the anomalies that could be carried out using either/both kinds of the previously discussed types. We grouped the anomalies discussed in the literature into twelve types. Table. 4 lists these anomalies and the major category they belong to. The anomalies are detailed further below.

Voids (A_{vd}): Voids or infill cavity occurs when a part in a printing process has an area where the material has been removed, e.g. by altering the G-code commands to the original file, such that the resultant geometry is the same but the mechanical properties are changed [26]. There are many factors involved in making each void attack specific and unique, such as the location, number, size, and shape of the void [47]. If these factors are considered not at random but targeted to object geometry can impart significant damage, and lead to critical part premature failure [10]. Zeltmann et al. [40], studied different sizes of void defects and their effect on the printed object strength. They concluded that a defect of a magnitude as low as $150um$ can significantly change part mechanical properties. Detecting such low-magnitude voids is a difficult research problem as these variations can lie within the normal printer specification tolerances [24].

Filament Density (A_{fd}): Filament density anomalies are the result of adversarial changes in the extruder feed rate of the printing process. In case of a lower-than-expected feed rate, the extruder nozzle might not extrude (jammed state) or partially extrude resulting in under-extrusion and if the feed rate is higher than expected it will result in over-extrusion. Rais et al. [11] discussed different variations such as enforcing cavity and varying density through filament speed and state (on/off). From the stealthiness point of view, these anomalies could be made to create an impact without changing object dimensions, print time, or weight of the targeted object and is obfuscated in the final print. Pearce et al. [23] demonstrated that by using filament kinetics for material reduction or relocation the tensile strength could be reduced by up to 50% of its designed value.

Print Speed (A_{ps}): Anomalies due to the malicious/non-optimized changes made in the speed of the print head, contribute to under/over-extrusion conditions [27]. An adversary can vary the print speed of some of the commands at specific layers [38], and compensate elsewhere to obfuscate the anomaly. Gao et al. [36] showed the effect of adverse nozzle speed across shells (outer walls) and infill layers, resulting in under-extrusion in the corresponding attacked layers of the print geometry.
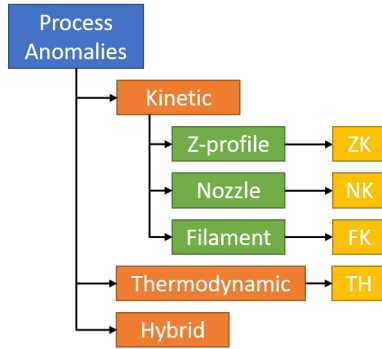
Figure 3. Process Anomalies Domains

Toolpath Manipulation (A_{tm})**:** These are malicious manipulation in the G-code to modify properties of the object and could be executed by insertion, deletion, modification, and re-ordering of the instructions [28]. An adversary could e.g., modify toolpath instruction to change extruder speed, or movement command along nozzle (X/Y) axis [25] or delete instructions that prints material at critical location [28]. Modification of G-code commands such that changing move pr instruction with just move alone will add smart voids in the part geometry [24]. Atomic toolpath manipulations (one command change) as investigated by Belikovetsky et al. [25] are difficult to detect and therefore need careful consideration for designing monitoring techniques.

Infill Anomaly (A_{if})**:** Due to affiliation with movement parameters, these process anomalies are categorized as kinetic. Infill plays a critical role in defining the mechanical properties of the print object [48]–[50]. Adversaries could therefore add malicious changes in these parameters resulting in degraded mechanical performance. For example, changing the infill angle from 45 to 30 degrees [40] or changing density from 100 to 75% [41]. Different variations of such attack defects have been simulated by Wu et al. [30], [31] by changing the original design file with a malicious one. Similarly, Bayens et al. [29] discussed the adverse effects of changing infill pattern and density for sabotaging a prosthetic knee implant.

Thermodynamic (A_{th})**:** These anomalies are related to malicious changes in the nozzle temperature [36], print bed temperature [38], and/or fan speed [36]. Xio [12] in the XCon information security conference 2013, showcased a practical demonstration for RepRap 3D printer using open source firmware. The developed exploit was able to automatically download the firmware, manipulate the temperature-related data and upload it back to the printer. Using the exploit, the nozzle temperature was manipulated to half of its intended value thereby affecting the print geometry. Similarly, Gao et al. [36] showed how changing fan speed from its original rate could potentially result in adverse effects on print geometry.

Z-Profile (A_{zp})**:** Categorized as kinetic, the layer thickness of a print object is dictated by z-axis movement. Layer thickness plays an important factor in defining the mechanical properties of a print [51]. Even targeting some of the layers [32], [34], [35] could do critical damage to the object. Rais et al. [38] presented different variations going as low as 0.1 mm change in thickness. Such attacks are subtle in nature and hence difficult to detect through visual inspection but can significantly reduce part strength.

Geometry (A_{gm})**:** The shell defines the outer geometry of the printed object and is internally supported by infill. An adverse change to kinetic and thermal parameters could lead to variations in part geometry. Maintaining dimensional accuracy is an important characteristic for defining a good-quality print. Rais et al. [38] presented 0.3mm dimensional changes in a single axis of the print geometry. Such negligible changes if added to an object, to be used as a critical component in an assembly, could lead to incompatible form and fit, and may also cause unusual excessive wear and premature failure. Factors such as shrinkage and warpage due to internal thermal stresses cause deformations in the geometry. Printing parameters like extruder temperature, and raster width if optimized can improve dimensional accuracy [52]. Dry printing due to material run-out or nozzle clogging, premature job termination, and print bed temperature are other contributors to dimensional irregularities.

Surface Quality (A_{sq})**:** Measured in terms of surface roughness, surface quality is influenced by many printing parameters [53]–[55]. Kumar et al. [53] studied parameters like layer thickness, raster angle, etc., and used the Taguchi design of experimental evaluation to estimate their role in defining surface roughness. Using the same technique Martinez et al. [54] evaluated layer thickness, inclination, and rotation along the z-axis as contributors to surface quality. Their prediction model gives a good approximation of the final surface roughness prior to the part being printed. Under/over-fill is another contributor to defining the surface quality of a 3D print [56]. Therefore, monitoring surface roughness within design specifications is critical for satisfactory printing results.

Warpage (A_w)**:** Warping in the printed geometry is the result of thermal stresses during the printing process. These stresses are due to the material having higher mechanical resistance and low thermal expansion resulting in shrinkage and hence warp effect [57]. Using adhesive at the print bed and closed chamber printing has been found to minimize the warpage defects [58]. Parameters like print size and layer thickness as a contributor to the warping effect have been investigated by Armillotta et al. [59]. They presented an analytical model for the evaluation of these parameters and their influence on warpage. Similarly, Panda et al. [60], studied the effect of four printing parameters; line width compensation, print speed, layer thickness, and extrusion rate, and quantified them for their influence on warping using a proposed evolutionary system identification (SI) approach. The results indicate that layer thickness and extrusion rate influence warpage the most than any other parameter.

Bonding (A_b)**:** Poor interlayer and first-layer bonding (adhesion with print bed) lead to degraded mechanical performance and material peeling off respectively. Interlayer bonding refers to the bonding of the previous layer with the new layer. Factors such as nozzle temperature and speed, print bed temperature, extrusion feed rate and temperature, and distance between the extruder and print have been studied to have a significant effect on bonding properties [61]–[65].

Extruder State (A_{es})**:** While the extruder conditioning itself is not attributed to the print quality but is associated with the printer's health and should therefore be

monitored for any anomalous behavior. Extruder monitoring covers the extruder's cold/hot end and the print nozzle. The cold end states include filament loading, unloading, and material runout conditions while the extruder hot end and nozzle states include normal, partially, or fully clogged conditions [6]. Printing parameters like nozzle temperature and filament feed rate directly affect the extruder state. Any adversarial changes to these parameters could completely clog the nozzle making the printer services unavailable or partially clog it to sabotage print.

6. Systematization of Knowledge

The following subsections detail the research efforts in both cybersecurity and QA domains, for real-time monitoring of process anomalies, along with the side channels and techniques they have employed for the purpose.

6.1. Acoustic (SC_A)

Acoustic emissions (AE) from the printing process can detect kinetic anomalies by identifying variations in control parameters such as axes, extruder speed, displacement, etc. as detailed below.

Filament Density (A_{fd})**:** AE signals were investigated by Li et al. [66] to classify different filament conditions. The AE data is collected and trained on deep learning **(M1)** algorithm named AE deep time convolution neural network (AETCN), with a detection accuracy of 98%. The technique however has low precision, as AE signals needed for analysis are only detected when distortion is large enough to touch the nozzle.

Print Speed (A_{ps})**:** Chhetri et al. [27] modified the printer firmware to add anomalous changes to nozzle speed. By training a regression model **(M1)** on acoustic data, they were able to achieve a detection accuracy of 73% for a change of 200 mm/min in speed parameter.

Toolpath Manipulation (A_{tm})**:** To verify 3D printed object integrity, Belikovetsky et al. [25] used fingerprinting method by generating a master audio profile and validating the printing process by checking it for similarity **(M4)**. Different thresholds were proposed and evaluated using modifying, inserting, replacing, and deleting a single G-code command. The correlation of audio signatures was studied to detect any malicious changes. While the proposed scheme can identify as minimum as a single G-code instruction change, it however is limited by factors like time synchronization and the inability to detect filament extrusion and temperature changes.

Infill (A_{if})**:** Acoustic signatures from a printing process compared with a master profile can help detect design discrepancies. Bayens et al. [29] proposed a 3-layer framework using acoustic and inertial sensors, and material analysis through spectroscopy. The acoustic signatures were captured and compared **(M4)** to verify the built geometry. A case study of malicious print of a prosthetic knee was used to detect infill pattern and density from Honeycomb to Rectilinear fill-pattern with 100% accuracy and is verified using post-production CT-scanning.

Warping (A_w)**:** Acoustic signal and accelerometer data were used to train SVM **(M1)** for accurately predicting the failure state of the printer process. Combining

AE with temperature data has been proposed by Nam et al. [67] to detect faulty prints due to first-layer adhesion and warping defects. Using non-linear SVM **(M1)** the technique was able to achieve detection accuracy of up to 100% but with limited precision for detecting such defects.

Bonding (A_b)**:** AE produced due to material striking or rubbing against the nozzle can help detect surface defects produced as a result of material stacking and first-layer bonding defects. Yu and Wang published a series of papers on using acoustic data for diagnostic purposes [66], [68]–[74]. AE features were used in their approach to identifying normal and failed printing processes. In the proposed approach [68], [72], [73], they have used AE hits to diagnose first-layer bonding defects. ML algorithms **(M1)** such as K-means clustering [68], hidden semi-Markov model (HSMM) based state vector machine (SVM) [72] and self-organizing map (SOM) [73] were used to train the model and identify different failure modes including material peeling off, buckling, dragging, and scratching with the nozzle.

Extruder State (A_{es})**:** AE hits can also help identify different extruder states i.e. normal, semi-blocked, blocked, loading, and material runout [69]–[71]. ML algorithms **(M1)** SVM [69], HSMM [70] and clustering by fast search and find of density peaks (CFSFDP) [71] were used for training and getting prediction results for different extruder states. The compressed sensing (CS) technique can reduce the required data and sensors for monitoring physical processes, as managing their number is challenging due to increased cost and processing capabilities. Lu et al. [75] employed CS and used AE hits and a physics-based constrained dictionary learning scheme to reconstruct the original signal using fewer data points. They classified **(M1)** different nozzle conditions with only 4% error while using as little as 40% of the original data.

Filament breakage due to nozzle clogging or other failures can be identified using AE signals. Yang et al. [76] proposed a mathematical and experimental approach **(M3, M4)** wherein they identified AE signals to have different probability distributions after breakage. The results indicate that instantaneous skewness could be used as an indicator for detecting broken filament.

6.2. Electric Current (SC_I)

Power signals, as a function of electric current, can provide information about the kinetics of the printing process. The printer nozzle (x/y-axis), print bed (z-axis), and extruder (e-axis) are all driven by stepper motors. Any anomalous behavior in them can therefore be monitored.

Filament Density (A_{fd})**:** Using a conductive material, Parker et al. [77] characterize the print by sending electrical signals and creating an in-situ resistance profile **(M4)**. The profile is then investigated for successfully predicting defects due to under/over-fill conditions.

Toolpath Manipulation(A_{tm})**:** The consumed electric current is the function of G-code commands. Therefore, any unaccounted manipulations will correspondingly affect the power consumption pattern. Gatlin et al. [24] used a master profile containing the electric current signature generated during the printing process compared with the in-process signals. The technique uses a set threshold **(M3)** to trigger alerts and is validated over four types of

command manipulations. Similarly, Rott et al. [28] uses deep learning to detect adversarial changes by predicting power signatures based on object design and previous electric current consumption behavior. Deep neural network (**M1**) is trained using power signatures of multiple toolpath instructions to predict power signatures. Different defects were injected to test the proposed system maintaining a detection accuracy of 96% with 95% precision.

Extruder State (A_{es}) Measuring extruder motor power could help predict the status/condition of the print head. Blocked or partially blocked condition decreases the nozzle's effective diameter causing increased resistance to flow, resulting in electric current variations. Kim et al. [78] studied the effect of nozzle condition in relation to the extruder motor and verified the hypothesis that a jam in the extruder would result in increased power drawn. Tlegenov et al. [79] presented a theoretical model (**M3**) for process forces in filament extrusion and the effect of nozzle clogging on extruder motor current. The model verified using experimental shows a non-linear increasing trend (**M4**) of electric current in relation to nozzle clogging.

6.3. Thermal (SC_T)

Thermal cameras and sensors, for monitoring the heat signature and temperature parameters respectively, are the two main techniques employed to detect bonding strength (A_b) and extruder conditioning (A_{es}) in the literature.

Thermodynamics (A_{th})**:** Using multiple sensors to monitor temperature distribution is proposed by Lu et al. [80]. Physics-Based compressive sensing (PBCS) was used to restrict high-volume data requirements and hence reduce computation costs. Using the methodology efficient and accurate monitoring of the printing process can be done with fewer sensors and computation requirements. The results indicate that only a few measurements such as from the side and top face were enough for a complete reconstruction of the 3D temperature profile. PBCS was further improved by introducing domain decomposition [81], [82] and boundary domain reduction [83] approach. The proposed method is then used for transient thermal distribution monitoring of the FFF process.

Bonding (A_b)**:** Thermal imaging has been investigated to detect any malicious/benign bonding anomalies (interlayer and first-layer). A proof of concept for the in situ process monitoring using the thermal channel is presented by Ferraris et al. [84]. Using an experimental numerical approach (**M4**), the signatures were compared in the time domain and a correlation is found between the acquired temperature profile with interlayer bonding. Pollard et al. [61] studied the effect of extruder feed rate on the interlayer bonding strength with the temperature recorded through thermistors and an IR camera. They concluded that a sudden decrease in extruder feed rate could cause structural weakness due to lower extruded temperature and hence result in lower bonding. In line with these results, Costa et al. [62] in addition to extrusion feed rate investigated more process parameters including, filament dimensions, sequence of deposition, and environment temperature to predict adhesion in between layers.

Seppala et al. [63]–[65] publish multiple articles on optimizing the interlayer bonding strength. Using an infrared (IR) camera to gather temperature profiles [63], they

showed that the material and printing process parameters correlate to the part strength, and understanding these temperature profiles is the first step to optimizing the bonding strength. Printing variables such as print head temperature and nozzle speed [64], extruder feed rate, and temperature [65], as a function of the weld zone temperature profile were investigated. Samples were printed over a range of these variables while gathering temperature profiles using an IR camera. Following a mathematical and experimental trend analysis (**M4**) they concluded that these variables contribute to the interlayer bonding strength of the material and should be optimized. Similarly, Malekipour et al. [85] investigation of temperature profile (**M3**) and temporal plot reveal that ambient temperature, infill density, and pattern also affect the thermal evolution of build layers. In addition to the thermal optimization of these process parameters, Prajapati et al. [86] investigated the standoff region between the nozzle tip and print bed and presented an analytical model (**M3**) to minimize temperature drop.

Understanding the effect of process parameters on thermal field evolution is important for ensuring quality in FFF. Li et al. [87] presented a framework for integrating physical printing parameters with a data-driven approach to enable quasi in-situ layer-by-layer thermal field prediction. With cross-validation, they concluded that using the proposed framework thermal field prediction could be done more accurately and efficiently. Caltanissetta et al. [88] used the same approach wherein using thermal camera layered thermal profile is developed to investigate spatiotemporal evolution (**M4**). They further investigated, anomalous thermal profiles due to hot and cold spots, contributing to interlayer bonding defects.

Extruder State (A_{es})**:** Thermal imaging can also help give information on the nozzle working status such as under/over-extrusion, warping, and normal printing state, an approach investigated by He et al. [89] and further extended by Hu et al. [90] using an IR camera to take thermal images of each layer and extract features. The features are compared using qualitative trend analysis (**M4**) [89] to build a knowledge base for finding the starting of each phase of nozzle conditions and using multi-class SVM (**M1**) [90] to classify nozzle states.

6.4. Optical (SC_O)

Optical SC uses cameras and scanners to gather process information. Cameras are put at a certain angle and distance to capture images or video for later analysis to monitor and find process-anomalies (A_{gm}, A_b, A_{fd}). Flatbed scanners on the other hand provide offline verification of the print to measure surface quality (A_{sq}).

Voids (A_{vd})**:** Mamun et al. [32], [33] proposed video-based printing process authentication. Using image processing (**M2**) and multi-linear principal component analysis (MPCA), their technique was able to detect void ($100mm^2$) and infill angle ($\pm 45°$) anomalies with up to 96% accuracy.

Filament Density (A_{fd})**:** Banadaki et al. [91] used videos to train Deep-CNN (**M1**) to quantify different under/over-extrusion conditions. The model is trained on each layer by extracting frames from the captured video. Increasing the speed and decreasing the temperature of the AM process lowers the quality and can result in

over/under-fill of material adding visible distortion on the surface or internal voids. The proposed model classifies the print as 5 levels of quality and achieves an accuracy of 94%. Jin et al. [92] uses CNN **(M1)** for detecting under/over-extrusion conditions, wherein in-situ video is captured and images are collected. The algorithm reached 98% accuracy in classifying print quality. Similarly, Zhang et al. [93] uses Deep-CNN **(M1)** to detect observable geometrical changes as a result of under/over-extrusion, warping, and first-layer bonding defects.

Baumann et al. [94] used image processing **(M2)** to detect defects due to filament kinetics and first-layer adhesion with a detection accuracy of up to 80% but is limited by high false positives. Liu et al [56] proposed an image-based closed-loop architecture that effectively classifies the surface images based on under/over-extrusion conditions. The architecture uses a digital microscope to collect images and extract features using textural analysis-based image processing **(M2)**. Classification algorithm **(M1)** trained on the features achieves an accuracy of 85%. A PID-based feedback system is then used to optimize the feed rate and temperature to achieve good surface quality.

Infill (A_{if})**:** Wu et al. [30], [31], uses machine learning **(M1)** algorithms to detect infill defects in the part geometry. Two types of camera assemblies, static and moving were used to capture images of the print object and train ML algorithms. The trained model was able to predict defects with up to 96% accuracy. Petsiuka et al. [95] proposed using G-code data to render a reference image and compare it with the actual print. Using HOG-based local image similarity **(M2)** and matrices to measure mismatch, they were able to detect defects like local infill, first-layer adhesion, and layer shifting at early print stages.

Geometry (A_{gm})**:** Optical cameras have extensively been investigated for detecting geometry/dimensionality variations. Augmented reality has been integrated by Ceruti et al. [96] to capture real-time print geometry and compared it with a virtual 3D model. Using image processing **(M2)** SURF algorithm, the two models are compared with error detection ranging above 1mm. The technique is limited by object geometry, with the feature recognizable by the SURF algorithm. Malik et al. [97] developed a Hololens application to enable layer-by-layer user inspection of the print geometry.

Straub [41]–[45], [98]–[100] used image processing **(M2)** and a multi-camera system to explore multiple printing defects. Per-layer images are compared with an ideal print or a CAD model to calculate the difference. However, the comparison result is affected by the alignment of the two geometries [100]. The proposed framework was explored for detecting attacks like positioning-based [42], infill level [41], and micro defects [43], which are of particular interest as visually challenging to inspection. Similarly, Nuchitprasitcha et al. [101], [102] proposed a 360-degree real-time optical monitoring platform to detect normal/failure printing state using image processing **(M2)**. The technique achieved a 100% detection rate for geometry variation >10%.

Instead of comparing with the CAD model or an ideal print, another approach is to convert the CAD model to a theoretical point cloud (PC) and find a correlation with the print geometry, a technique proposed by Kopsacheilis et al. [103]. The algorithm uses april tag to find the region of interest (ROI) and filter outliers. The correlation with the theoretical PC detects a spatial change in the print geometry by around 9.6%. Using a similar approach Charalampous et al. [104] used 3D scans, captured using a 3D light scanner, at regular intervals to construct real-time PC and compare it with corresponding theoretical PC **(M3)**. Instead of using ideal PC data, one can train the model with synthetic data containing aberrations. Li et al. [105] using the technique trained multiple ML algorithms **(M1)** and achieved detection accuracy of 98% with Bagging and Random forest models for detecting $3mm$ radii geometrical defects.

Statistical Process Control (SPC) flow charts have also been used for monitoring changes in the profile of the part geometry. Ketai et al. [106] and Ye et al. [107], [108] used the technique with the assumption that an abrupt change in geometry is observed in case of error. Images of each layer were collected and the contours were retrieved using image processing **(M2)**. The data is then analyzed using control flow charts and a signal is generated in case deviation in the profile is detected.

Surface Quality (A_{sq})**:** Contrary to using a CAD model or an ideal print for comparison, another approach is to use data-driven techniques. Okarma worked in collaboration with Fastowicz [109]–[125] proposed no-reference quality assessment of surfaces using image processing **(M2)**. Scanned images of flat surfaces were collected and correlations of variable distortion levels were found using different algorithms. As the distortion increases, the mutual similarity decreases. Based on this finding, different techniques such as structural similarity metrics [110], feature similarity metrics [112], mutual similarity [122], [123] and the combined matrix [124], [125] were proposed and evaluated for their effectiveness to detect distortion. Similarly, surface distortion increases the local image entropy [118]–[121], therefore, can help distinguish good/bad quality samples. An online approach for measuring the surface quality is proposed by Huang et al. [126]. Images of each layer are captured, while a control chart is used to signal mean shift deviation indicating a geometry defect. Blanco et al. [127] used flatbed scanners for contour verification using image processing **(M2)**. The technique is limited by the offline capturing/scanning of flat surfaces and therefore not suitable for real-time monitoring and for complex geometry structures.

Warpage (A_w)**:** Li et al. [128] proposed the use of coherent gradient sensing (CGS) technology for monitoring thermal stresses resulting in warping deformation. The experimental evaluation includes a PLA material specimen measured at three different cooling rates: fast, transient, and slow. The results show the effect of these rates on thermal residual stresses and the introduced deformations, indicating CGS feasibility for monitoring such defects.

Bonding (A_b)**:** Machine learning **(M1)** for training models and predicting warping defects (A_b) is proposed by Saluja et al. [129]. Deep learning Convolutional Neural Network (CNN) is used for training and testing, wherein, the data is collected by stopping the print at every layer for $2s$. The image is limited to the region of interest to reduce computation complexity. The proposed scheme was found to be 99.3% accurate in detecting warping defects.

Extruder State (A_{es})**:** Optical sensing could be used to monitor printer state. Greeff et al. [130] proposed a

closed-loop system for detecting and compensating defects due to filament feed rate. Filament slippage, which happens due to high feed rate and low extrusion temperature, is monitored by capturing and analyzing process video. Image processing **(M2)** is used to evaluate certain ROI and to estimate speeds. The calculated speeds were then analyzed **(M4)** for detecting and compensating feed rate in a closed loop thereby contributing to higher accuracy prints. Heras et al. [131] used an optical encoder to calculate filament speed and alert changes due to material runout, nozzle clogging, or filament breakage. A feedback loop in place then pauses the print in erroneous condition.

6.5. Laser (SC_L)

Limited literature is available on using laser SC and is focused on detecting geometry (A_{gm}), surface quality (A_{sq}), and layer thickness (A_{zp}) type anomalies.

Z-Profile (A_{zp}): A 2D laser triangulation scanning approach is presented by Faes et al. [132] wherein a camera in combination with a $650nm$ laser is used to detect dimensions i.e. thickness and width of the track. The setup was able to detect z-dimensional inaccuracies of up to $100um$. The technique, however, is limited by material color, since translucent materials reflect less light, because of a higher refractive index, resulting in larger inaccuracies in measurements.

Geometry (A_{gm}): Laser sensing provides high-resolution layer-by-layer geometry information which can be analyzed to detect anomalies. Li et al. [133] proposed the feasibility of using PC laser-scanning data for detecting abnormalities in print for simple and complex geometries. In the extension of their work [134] they used ML **(M1)** conditional adversarial network (CAN) models to predict scanned-PC using 3D CAD geometry. The predicted PC is then statistically compared with laser-scanned PC data to detect geometric inaccuracies.

Surface Quality (A_{sq}): Laser scanning approach has also been adopted to detect surface inaccuracies due to under/over-fill conditions. Lin [135] used scanned PC data of the print surface and compared it with the CAD model to detect surface defects. The three-stage method includes converting PC data to a 2D image, comparing the image with a CAD model using image processing **(M2)**, and defect reconstruction measuring the dimension and type of defect. The technique was able to detect an underfill of $4.6mm^3$ with an error of 13.5% and $6.6mm^3$ overfill with a 12.5% error.

6.6. Pressure (SC_P)

Pressure sensors have been employed to study nozzle conditioning (A_{es}) and optimize bonding (A_b) with some work on detecting warpage defects (A_w).

Warpage (A_w): Pressure readings on the extruder can indicate the presence of warpage defects. Moretti et al. [136] presented an approach in which upward-oriented force on the extruder during the printing phase is measured. The data is then processed using simulation software monitoring the part compliance and stiffness. The results indicate 93% accuracy in detecting warpage defects, for warpage significant enough to touch the extruder.

Bonding (A_b): Coogan et al. [137], [138] used in-line pressure, temperature, and viscosity measurements within printer nozzle for predicting interlayer bonding strength. The experimental results provide insights into the extrusion process, which can help optimize bonding strength and detect defects. The sensor data is used to plot and analyze **(M4)** continuous viscosity curve as a function of shear rate, temperature, and pressure. The results indicate that in-line rheometer viscosity data can be used to monitor and control the process.

Extruder State (A_{es}): Pressure side channel has been used to monitor nozzle behavior during the printing process. Anderegg et al. [139] presented a theoretical and experimental **(M3)** approach for modeling pressure and temperature distribution in the printer nozzle during idle and extrusion conditions. The study aims to provide improved process monitoring for detecting changes in flow rate leading to inconsistent extrusion conditions. Another such study is presented by Peng et al. [140] wherein using experimental method **(M3)**, the flow behavior and temperature history during the extrusion process is analyzed. To visualize the flow, inorganic pigments are selectively included in the filament as flow indicators to illustrate the flow history. The effect of temperature and feed rate on the filament distribution was profiled **(M4)**. The results indicate the extrusion process to be highly non-isothermic at high feed rates. The measurements provide critical data for understanding the printing process parameters.

6.7. Vibration (SC_V)

Vibrations during printing can provide valuable information about multiple physical aspects. Process anomalies such as filament density (A_{fd}), nozzle state (A_{es}), and layer-thickness (A_{zp}) have been studied in the literature.

Filament Density (A_{fd}): Bukkapatnam et al. [141] proposed using an accelerometer for monitoring process conditions including over/under-flow conditions due to sub-optimal feed rates. Five conditions including normal, underflow, overflow, fast, and slow feed rate were then categorized using a neural network **(M1)** model with the accuracy ranging up to 91% for variations >6%.

Z-Profile (A_{zp}): Data from MEMS accelerometers can also be used to train ML algorithms to detect kinetic anomalies. Shi et al. [34] proposed a data-driven feature extraction approach based on LSTM-autoencoders. MEMS accelerometers were used to gather data, wherein supervised [35] and unsupervised ML algorithms **(M1)** were employed to train the model on extracted features. An F-score of 96% shows that the method can effectively detect $100mm^2$ voids and layer thickness variations.

Extruder State (A_{es}): Vibration sensors have also been proposed to monitor anomalous nozzle conditions. Tlegenov et al. [142] proposed a physics-based model **(M3)** to represent the nozzle state during the printing process. As the moving extruder adds dynamic noise to the measurements, the MEMS accelerometers were mounted to an experimental setup with a fixed nozzle and moving bed. The results indicate acceleration amplitude increases non-linearly **(M4)** during nozzle clogging and hence can effectively monitor such printing conditions.

TABLE 5. SPECIFICATIONS OF COMMONLY USED PRINTERS IN LITERATURE

No.	Printer name	Cloud Enabled	Build Volume (cm)	No. of Extruders	Connectivity	Supported file type	Fimware
1	Ultimaker S3	Yes	23 x 19 x 20	2	USB, Ethernet, Wifi	STL, OBJ, X3D, 3MF, BMP, GIF, JPG, PNG	Marlin
2	MakerBot Replicator+	Yes	29.5 x 19.5 x16.5	1	USB, Ethernet, Wifi	STL, OBJ	Custom
3	LulzBot Taz 6	No	28 x 28 x 25	2	USB	STL, OBJ, X3D, 3MF, JPG, PNG	Marlin
4	Prusa i3 MK3S	Yes	$25 \times 21 \times 21$	1	USB, Ethernet, Wifi	STL, OBJ, AMF, 3MF	Marlin
5	PrintrBot Plus	No	25 x 25 x 26.5	1	USB	STL	Marlin
6	Hyrel 3D E5	No	20 x 20 x 20	1	USB	STL	Hydra

6.8. Heterogeneous Sensors (SC_H)

Using multiple sensors for monitoring different process parameters for detecting anomalous behavior is another approach used by researchers. Sensors like accelerometer, encoders, thermocouples, etc. combined gives a comprehensive knowledge of the process.

Voids (A_{vd})**:** Yu et al. [26] proposed a multi-modal system for detecting voids. Using analog emissions from multiple SCs as a dataset, ML models (**M1**) were trained to find the estimation function. In the testing phase real control signals are then compared with values from the estimation function, wherein a mismatch indicates anomalous behavior. The proposed system is evaluated by detecting void, adding 15% deviation in the design geometry, with achieved detection accuracy of 98%.

Surface Quality (A_{sq})**:** Rao et al. [143] presented an approach wherein data from heterogeneous sensor arrays are used to detect failure using a nonparametric bayesian Dirichlet process model and evidence theory (**M3**). Effects of printing variables i.e. feed rate, extruder temperature, and layer height on surface roughness were studied. The model is trained on the data collected from the thermal and vibration sensors attached to the print bed and extruder. The model achieved an average F-score of 85% in classifying normal, abnormal, and failure extrusion conditions by measuring surface roughness of up to $6.5um$. In the extension of their work [144] online sparse estimation-based classification (OREC) was used and achieved an F-score of 90% in determining filament kinetics abnormalities.

Multiple Anomalies: Using data from multiple SCs researchers have attempted to monitor multiple process anomalies. Gao et al. [36] for example explored four categories of anomalies including void (A_{vd}), nozzle kinetic (A_{ps}), layer thickness (A_{zp}), and fan cooling attack (A_{th}). By acquiring data from the accelerometer, magnetometer, and camera, and applying mathematical modeling (**M3**) and image processing (**M2**), they were able to achieve 97% accuracy in detecting significant distortions in the part geometry due to fan cooling. They also obtained a mean absolute error of 6.07% and 9.57% for speed and layer thickness estimation, respectively.

An alternative to training ML models is to use sensor data and compare it in real-time with an ideal profile. Liang et al. [39] proposed the use of dynamic synchronization to tolerate time noise and compare two signals. Employing a data acquisition system to collect six different side-channel signals, the proposed anomaly detection approach gives 99% detection accuracy in detecting void (A_{vd}), 5% change in speed (A_{ps}), infill (A_{if}) pattern change, 0.3mm layer thickness (A_{zp}) and up to 5% geometry (A_{gm}) deviations.

While using a multi-channel detection approach provides a good estimation of the printing process, subtle changes to the printing parameters could potentially go unnoticed. These aberrations, though small, can still affect part geometry strength. Rais et al. [38] proposed Sophos, a modular framework to detect minimal deviations across the complete threat surface ($A_{vd} - A_g$). In its implementation using optical encoders, thermocouples, and thermistors, they were successfully able to detect 16 kinetic, thermodynamic, and hybrid attacks. By transforming G-code instructions through spatiotemporal modeling, and comparing them with the sensors data, the attacks were detected on the layer they occur.

7. Discussion

This section presents the analysis of the current research trends, and challenges associated with each SC, followed by future recommendations.

7.1. Analysis

A list of printers, along with their technical details, that are commonly used by the majority of researchers is presented in Table 5. A few printers support multiple extruders, however, we do not find much research literature exploring the impact of extruder switching attacks on the side channels' performance. Most of the printers used in the literature use open-source firmware, Marlin. Thereby, enabling researchers to use firmware to augment their attack detection scheme in a consolidated framework.

The accuracy and precision of an SC for the detection of process anomalies are important in designing a monitoring scheme. Table 6 lists the achieved accuracy (Acc) and precision (Prec) of different SCs in the literature. The table summarizes the highest achieved Acc and Prec using a particular SC for the detection of a targeted process anomaly. Most of the reviewed articles don't provide the precision and/or accuracy of their proposed technique and are therefore not listed in the table. Due to the lack of such details, it becomes challenging to compare one technique with the other. However, the general trend in the table strongly suggests that Heterogeneous Sensors (SC_H) are found to be highly precise and accurate for detecting most of the process anomalies. Similarly, the acoustic side channel (SC_A) achieves more accuracy in detecting different extruder conditions (A_{es}) i.e. up to 4 different states with 98% accuracy. Figure 4 details two key linkages identified through a systematic review of the literature; association of SCs for identification of process anomalies and printing parameters contributing to these anomalies. Based on these findings a generic framework enabling researchers in designing/implementing a monitoring system is detailed in Appendix A.

TABLE 6. PRECISION (PREC) AND ACCURACY (ACC) OF SIDE CHANNELS FOR DETECTION OF PROCESS ANOMALIES (A)

SC	A_{vd} Prec	Acc	A_{fd} Prec	Acc	A_{ps} Prec	Acc	A_{tm} Prec	Acc	A_{if} Prec	Acc	A_{th} Prec	Acc	A_{zp} Prec	Acc	A_{gm} Prec	Acc	A_{sq} Prec	Acc	A_w Prec	Acc	A_b Prec	Acc	A_{es} Prec	Acc
SC_A	–	–	200 mm/min [27]	73	– [66]	98	1 cmd [25]	100	– [29]	100	–	–	–	–	– [145]	87.5	–	–	– [72]	96	– [72]	96	4 states [71]	98
SC_I	– [24]	100	– [24]	100	– [28]	96	1 cmd [24]	100	– [24]	100	–	–	– [24]	100	– [24]	100	–	–	–	–	–	–	– [79]	8 ER
SC_T	–	–	3°C [90]	87.5	–	–	–	–	–	–	– [80]	6.86 ER	–	–	–	–	–	–	–	–	–	–	4 states [90]	87.5
SC_O	100mm² [35]	96	50% [56]	85	–	–	–	–	15° [32]	96	–	–	–	–	3mm [105]	98	50% [56]	85	– [129]	99	–	–	–	–
SC_L	–	–	[56]	>3 ER	–	–	–	–	–	–	–	–	– [132]	0.1mm ER	0.15mm [134]	99	4.6mm³ [135]	13.5 ER	–	–	–	–	–	–
SC_P	–	–	–	–	–	–	–	–	–	–	–	–	–	–	–	–	–	–	– [136]	93	–	–	–	–
SC_V	100mm² [35]	96	>6 [141]	91	–	–	–	–	–	–	–	–	0.05mm [35]	96	–	–	–	–	–	–	–	–	–	–
SC_H	1mm² [38]	100	1% [38]	100	≥2sec [38]	100	>1mm [38]	100	1% [38]	100	5°C [38]	100	≥ 0.05mm [38]	100	2% [38]	100	6.5um [143]	85	– [67]	100	– [67]	100	–	–

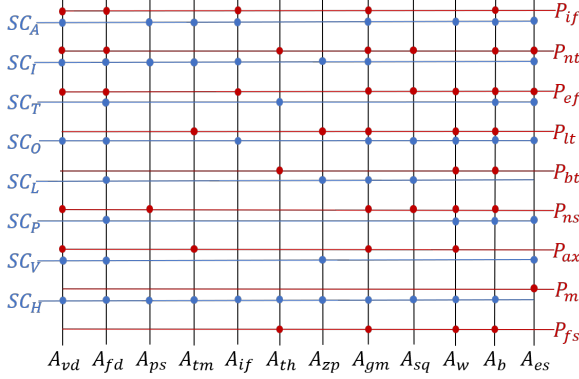
Figure 4. SC linkages for detection of process anomaly (A) and associated printing parameters (P)

TABLE 7. LIMITATIONS AND CHALLENGES ASSOCIATED WITH SCs

Side Channel	Scope	Intrusivity	Noise Sensitivity	Calibration Complexity
SC_A	FK, NK, ZK	No	High	High
SC_I	FK, NK, ZK	Yes	Low	Low
SC_T	TH	No	Medium	High
SC_O	FK, NK, ZK	No	High	High
SC_L	FK, NK, ZK	No	Medium	Medium
SC_P	FK	Yes	Low	Medium
SC_V	NK	No	Medium	Low
SC_H	FK, NK, ZK, TH	No	Low	Low

Table 8 summarizes in-situ monitoring and anomaly detection techniques. The literature is grouped based on the requirement of the master profile and the acquisition techniques/ side channels. Each paper is summarized based on the methodology used to find a correlation between the data obtained through SC, monitored process anomalies (A), and the research domain i.e. quality assurance (Q) and security (S). Looking at these statistics Optical (SC_O) was found to be the most extensively used, with heterogeneous sensors (SC_H) covering most of the process anomalies. Geometry (A_{gm}) process anomaly is the most explored, while toolpath manipulation (A_{tm}) is the most under-explored process anomaly in the literature.

Available studies for monitoring process anomalies using SCs are more frequent in the QA domain with only a few available in the security domain. However, the literature study revealed a trend in evaluation criterion, where the detection of process anomaly in QA generally has low precision than security techniques monitoring the sabotage of the print object. On the other hand, the QA domain covers a broader feature set e.g warping, surface roughness, interlayer bonding, and extruder conditioning along with other process anomalies. QA process monitoring techniques mostly focus on finding one type of process anomaly at a time, whereas, in security, researchers attempt to cover most of the anomaly surface.

Although both QA and cybersecurity researchers use side channels, there is a fundamental difference in their approaches. Cybersecurity research is deception-focused, whereas QA research is quality-focused. QA domain primarily targets the printed part, whereas cybersecurity research aims to identify any intrusion or malicious modification in the printing process. Topics like optimization of printing parameters are seen in the QA side channel literature only. On the other hand, cybersecurity researchers try to establish the integrity of the printing process, irrespective of the impact on the printed part.

7.2. SC Limitations and Challenges

Each side channel due to its intrinsic nature has different research challenges and limitations associated with them. To effectively discuss them in relation to each SC we considered four parameters as detailed below:

- **Scope** defines which physical domain (FK, NK, ZK, TH) of the printing process the literature is majorly focused on and is influenced by SC's intrinsic limitation or accuracy in measuring them.
- **Intrusiveness** states if the physical process is being manipulated/retrofitted to take measurements.
- **Noise Sensitivity** defines variability in SC data triggered by variable environmental conditions.
- **Calibration complexity** explains how difficult is to collect interpretable data from SC under different printers/printing environments.

Table 7 lists these parameters and the interpretation of these to each SC is detailed further.

Acoustics (SC_A) emanations are limited to monitoring process variables that produce sound during the printing and are therefore more effective in monitoring kinetic anomalies. AE data could easily be gathered by placing a microphone near the printer and is therefore non-intrusive in nature. However, the SC's accuracy is highly sensitive to environmental noise in the data and should therefore be pre-processed. Also, different printers and printing environments produce different frequency sounds corresponding to complex calibration requirements.

Electric current (SC_I) is more effective in detecting kinetic anomalies since the thermal process consumes proportional current but cannot provide complete information alone. The data is less sensitive to environmental noise,

TABLE 8. SUMMARY OF IN-SITU MONITORING AND ANOMALY DETECTION TECHNIQUES

Profiling	SC	Ref.	Printer	Method-ology	Q/S	A_{vd}	A_{fd}	A_{ps}	A_{tm}	A_{if}	A_{th}	A_{zp}	A_{gm}	A_{sq}	A_w	A_b	A_{es}
Per-Object Profiling	SC_A	[25]	Replicator, PrintrBot Plus, BCN3D Sigma	M4	S					✓							
	SC_I	[27]	printrbot	M1,3	S				✓								
		[29]	Lulzbot Taz6, Lulzbot TazMini, Orion Delta	M4	S					✓							
		[24]	Printrbot Plus	M3	S	✓	✓	✓	✓	✓		✓	✓				
		[28]	Lulzbot Mini	M1	S	✓			✓	✓							
	SC_T	[90]	Makerbot	M1	Q		✓										✓
	SC_O	[127]	BCN3D Sigma	M2	Q								✓				
		[96]	Replicator 2x	M2	Q								✓				
		[42], [43], [44], [98], [45], [99]	Replicator 2	M2	S								✓				
		[41]	Replicator 2	M2	S					✓							
		[101], [102]	RepRap Delta	M2	Q								✓				
		[95]	RepRap Delta	M2	Q					✓						✓	
		[146]	MakerBot M2	M2	Q										✓		
		[129]	Prusa i3 MK2S	M1,2	Q											✓	
		[97]	Prusa i3 MK3	M2	Q								✓				
		[103], [104]	Ultimaker 3x, Prusa i3 MK3S	M2	Q								✓				
		[105]	Replicator 2x	M1	Q								✓				
		[92]	Prusa i3 MK3	M1	Q		✓										
		[93]	Ultimaker 3	M1	Q		✓						✓		✓		
		[91]	Creality3D, Ender-3	M1	Q		✓										
		[32], [33]	Prusa i3 MK3S	M2	S	✓				✓							
		[56]	Hyrel 30M	M1,2	Q		✓							✓			
		[30], [31]	Replicator 2	M1	S					✓							
		[147]	Lulzbot Mini	M1,2	Q									✓			
	SC_L	[133], [134]	Hyrel 30M	M1	Q								✓				
		[135]	Exp. Setup	M2	Q		✓							✓			
	SC_V	[141]	Exp. Setup	M1,3	Q		✓										
		[34], [35]	Prusa i3 MK3S	M1	S	✓						✓					
	SC_H	[39]	Ultimaker 3	M3,4	S	✓		✓		✓		✓	✓				
		[26]	Ultimaker 3	M1	S	✓		✓									
Per-Setup Profilling/ No Profilling	SC_A	[68], [72], [73], [74]	Hyrel 3D E5, D-force delta bot, Z-630S JG Aurora	M1	Q										✓	✓	
		[69]–[71]	Hyrel 3D E5	M1	Q												✓
		[66]	NA	M1	Q		✓										
		[94]	Replicator 2x	M2	Q		✓									✓	
		[75]	Hyrel 3D	M1	Q												✓
		[76]	Stratasys uPrint, JG Aurora	M3,4	Q												✓
		[145]	Ultimaker 2	M1	Q								✓				
	SC_I	[78]	FDM 3000	M4	Q												✓
		[77]	Exp. Setup	M4	Q		✓										
		[79]	Replicator	M3,4	Q												✓
	SC_T	[62]	Exp. Setup	M4	Q											✓	
		[61]	Bulldog Extruder	M4	Q											✓	
		[63]–[65]	Replicator 2x	M4	Q											✓	
		[84]	Prusa MK3	M4	Q											✓	
		[87]	Orion Delta	M3,4	Q											✓	
		[88]	Exp. Setup	M2,4	Q											✓	
		[85]	Air Wolf	M4	Q											✓	
		[86]	Exp. Setup	M3,4	Q											✓	
		[80]–[83]	Hyrel 3D	M2,3,4	Q							✓					
		[89]	Makerbot	M4	Q		✓										✓
	SC_O	[109]–[125]	Prusa i3, RepRap Pro	M2	Q									✓			
		[106]–[108]	Flash Cast Creator	M2	Q									✓			
		[131]	Prusa i3	M4	Q		✓										✓
		[130]	Renkforce RF1000	M2,4	Q		✓										✓
		[128]	NA	M4	Q										✓		
		[126]	Hori Z300	M2	Q									✓			
	SC_L	[132]	NA	M2	Q							✓					
	SC_P	[139]	Maker Select	M3,4	Q												✓
		[140]	Cartesio 3D	M3,4	Q		✓										
		[137], [138]	Lulzbot Taz 6	M3,4	Q											✓	✓
		[136]	Exp. Setup	M4	Q										✓		
	SC_V	[142]	Replicator	M3,4	Q												✓
	SC_H	[36]	Ultimaker 2, Lulzbot Mini	M3,4	S			✓		✓	✓	✓					
		[38]	Ultimaker 3	M3	S	✓	✓	✓	✓	✓	✓	✓	✓				
		[143]	Replicator 2x	M3,4	Q		✓							✓			
		[67]	Ultimaker 2	M1	Q											✓	✓
		[144]	Replicator 2x	M3,4	Q		✓										

however, measurement is intrusive in nature as the sensing equipment needed to be placed in series. Calibration is relatively easy due to the availability of specifications of the printer parts, providing their characteristic behavior.

Thermal (SC_T) literature is constrained to monitoring interlayer bonding strength or nozzle conditioning. Thermal cameras could provide kinetic information, but they are not often explored due to the availability of more accurate sensing equipment, such as optical cameras. The SC is non-intrusive in nature with data accuracy mildly affected by environmental temperature variations. Thermal SC has higher calibration complexity due to physical/chemical variables such as material composition etc. affecting the material bonding properties.

Optical (SC_O) is non-intrusive, but lacks thermal data and is prone to inaccuracies due to lighting conditions, camera view obstructions, and difficulty in monitoring complex shapes. Proposed solutions include controlled lighting, lowering the print bed each layer, which adds to printing time and potentially affects the print thermal profile, and using multiple cameras, which adds to the calibration complexity. Moreover, real-time processing of large data becomes resource-intensive, making real-time verification of print geometry difficult.

Laser (SC_L) has been used to monitor kinetic anomalies and is non-intrusive in nature. However, scanned 3D online reconstruction for detecting geometric inaccuracies is limited by the noise in the PC data and the precision of the scanning equipment. Also, laser triangulation depends on the material type and color, as translucent material reflects less light, thereby resulting in information loss.

Pressure (SC_P) literature is limited to analyzing filament behavior. The sensing equipment is added by retrofitting the printer nozzle thereby increasing the calibration complexity of the setup. However, the data is resilient to the environmental noise factor.

Vibration (SC_V) is limited to kinetic anomalies with non-intrusive data collection. The data, however, is sensitive to external noise thereby limiting monitoring accuracy. The calibration complexity is low owing to the sensing data being easily mapped/interpretable to process.

Heterogeneous sensors (SC_H) provide more process information but processing and correlation of such large incoming data add to the computational complexity. While the fusion of data gives an opportunity to get more accurate results, a research challenge that arises with it is to give precedence to which SC data in case of conflicting verdicts to interpret a particular process anomaly.

7.3. Recommendations

Before designing and deploying monitoring techniques for a particular use case, factors such as sensor intrusiveness, precision, noise in data, environment variables, etc. should be taken into account. For example, a home consumer would be inclined to save material while compromising on the precision of the print object while an industrial setup may need to maintain precision and accuracy in the product and could discard a low-quality print.

In industry 4.0 where the parts are custom-made and changing frequently, having to train the monitoring techniques per object bases is inefficient. Therefore no-profile or per-setup profiling is where the research should be focused to mature these techniques. Similarly, there is little emphasis in the literature on the closed-loop monitoring and quality assurance of the FFF process. Modeling such a system is complex due to different factors, e.g. environmental conditions, material properties, etc., affecting the physical domain process. A self-correcting closed-loop process addressing these factors, however, could greatly improve the quality of the print object.

AM, as a new technology and fundamentally different from its predecessor, requires the labor force to adapt to new product engineering, designing, and production cycles. A skilled worker potentially aware of quality issues could tune the printing parameters accordingly. Since securing these systems needs in-process monitoring therefore workers should also be trained on security solutions to effectively identify sabotage attempts.

AM has the potential to lower its carbon footprint by manufacturing customized on-demand products with low wastages, decentralized manufacturing with high efficiency, and a shorter supply chain. However, with AM becoming accessible and affordable some security concerns like illegal production of weapons, counterfeit parts, and IP theft are ever-increasing. Therefore inbuilt security solutions such as watermarking [148] should be adopted to thwart such attempts. An adversary can attempt to gain access and exploit sensing data therefore the monitoring setup should be designed with security considerations.

Attacks are getting smarter and more obfuscated, to evade the monitoring schemes, by keeping the footprint below the detection horizon and can go as low as printer specification tolerances. Identification of such process anomalies could serve as a future research problem. The challenge is not only to detect low-magnitude deviations but also to disambiguate them with benign printing inaccuracies within the specifications to avoid false positives.

Since the goal of the monitoring schemes (QA/Security) in general is to maintain the print object performance specifications within the user-specified ranges, therefore monitoring as general should cover all discrepancies with the highest achievable precision to meet design criteria. To enable better comparative analysis, a benchmark of these techniques is necessary. This will make it more convenient for researchers to benefit from and build upon the available literature. For example measuring, surface distortion in terms of surface roughness, extruder conditioning by different states, and infill density changes by % difference. With the availability of such a standard framework, there comes an opportunity of benefiting from cross-domain knowledge to achieve high printing performance.

8. Conclusion

Due to its cyber-physical nature, AM process exhibits a variety of side channel that yields a reasonable estimation of the physical process. Different monitoring and anomaly detection techniques have been proposed in the literature to detect process anomalies using physical domain knowledge. This study presented an approach for systematizing knowledge based on identifying available SCs, and the acquisition and analysis methodologies. The approach uses eight different side channels to identify 12

types of process anomalies, chosen based on their use and availability in the literature. The accuracy and precision of an SC are essential for designing a monitoring scheme. The literature trend reveals that heterogeneous sensors are more precise and cover most process anomalies. Due to their intrinsic nature, each SC presents different challenges and limitations and is detailed in the study. The study identified commonalities and differences in the use of SCs for the domain of QA and cybersecurity. Cybersecurity is more deception-focused, while QA techniques are inclined toward quality. Recommendations were made to develop a common framework to benchmark the process monitoring techniques, anticipating opening cross-domain knowledge consumption and emphasizing collaboration opportunities.

Acknowledgement

References

[1] KBV Research, "Share & industry trends analysis report by type, by technology, by sales channel, by end-use, by regional outlook and forecast, 2021–2027," *ReportLinker: Lyon, France*, 2022.

[2] T. Wohlers and T. Gornet, "History of additive manufacturing," *Wohlers report*, vol. 24, no. 2014, p. 118, 2014.

[3] N. Gupta, C. Weber, and S. Newsome, "Additive manufacturing: status and opportunities," *Science and Technology Policy Institute, Washington*, 2012.

[4] GE Aviation. (2018) New manufacturing milestone: 30,000 additive fuel nozzles. [Online]. Available: https://www.ge.com/additive/stories/new-manufacturing-milestone-30000-additive-fuel-nozzles

[5] B. T. Wittbrodt, A. G. Glover, J. Laureto, G. Anzalone, D. Oppliger, J. Irwin, and J. M. Pearce, "Life-cycle economic analysis of distributed manufacturing with open-source 3-d printers," *Mechatronics*, vol. 23, no. 6, pp. 713–726, 2013.

[6] Y. Fu, A. Downey, L. Yuan, A. Pratt, and Y. Balogun, "In situ monitoring for fused filament fabrication process: A review," *Additive Manufacturing*, vol. 38, p. 101749, 2021.

[7] M. Yampolskiy, W. E. King, J. Gatlin, S. Belikovetsky, A. Brown, A. Skjellum, and Y. Elovici, "Security of additive manufacturing: Attack taxonomy and survey," *Additive Manufacturing*, vol. 21, pp. 431–457, 2018.

[8] A. E. Elhabashy, L. J. Wells, J. A. Camelio, and W. H. Woodall, "A cyber-physical attack taxonomy for production systems: a quality control perspective," *Journal of Intelligent Manufacturing*, vol. 30, no. 6, pp. 2489–2504, 2019.

[9] D. A. Brion, M. Shen, and S. W. Pattinson, "Automated recognition and correction of warp deformation in extrusion additive manufacturing," *Additive Manufacturing*, vol. 56, p. 102838, 2022.

[10] S. Belikovetsky, M. Yampolskiy, J. Toh, J. Gatlin, and Y. Elovici, "dr0wned–{Cyber-Physical} attack with additive manufacturing," in *11th USENIX Workshop on Offensive Technologies (WOOT 17)*, 2017.

[11] M. H. Rais, Y. Li, and I. Ahmed, "Dynamic-thermal and localized filament-kinetic attacks on fused filament fabrication based 3d printing process," *Additive Manufacturing*, vol. 46, p. 102200, 2021.

[12] C. Xiao, "Security attack to 3d printing," *xFocus Information Security Conference*, 2013.

[13] J. Gatlin, S. Belikovetsky, Y. Elovici, A. Skjellum, J. Lubell, P. Witherell, and M. Yampolskiy, "Encryption is futile: Reconstructing 3d-printed models using the power side-channel," in *24th International Symposium on Research in Attacks, Intrusions and Defenses*, 2021, pp. 135–147.

[14] C. Song, F. Lin, Z. Ba, K. Ren, C. Zhou, and W. Xu, "My smartphone knows what you print: Exploring smartphone-based side-channel attacks against 3d printers," in *Proceedings of the 2016 ACM SIGSAC Conference on Computer and Communications Security*, 2016, pp. 895–907.

[15] M. A. Al Faruque, S. R. Chhetri, A. Canedo, and J. Wan, "Acoustic side-channel attacks on additive manufacturing systems," in *2016 ACM/IEEE 7th international conference on Cyber-Physical Systems (ICCPS)*. IEEE, 2016, pp. 1–10.

[16] S. R. Chhetri, A. Canedo, and M. A. A. Faruque, "Confidentiality breach through acoustic side-channel in cyber-physical additive manufacturing systems," *ACM Transactions on Cyber-Physical Systems*, vol. 2, no. 1, pp. 1–25, 2017.

[17] M. A. Al Faruque, S. R. Chhetri, A. Canedo, and J. Wan, "Forensics of thermal side-channel in additive manufacturing systems," *University of California, Irvine*, vol. 12, no. 13, p. 176, 2016.

[18] S. Liang, S. Zonouz, and R. Beyah, "Hiding my real self! protecting intellectual property in additive manufacturing systems against optical side-channel attacks," in *Network and Distributed System Security (NDSS) Symposium*, 2022.

[19] S. R. Chhetri and M. A. Al Faruque, "Side channels of cyber-physical systems: Case study in additive manufacturing," *IEEE Design & Test*, vol. 34, no. 4, pp. 18–25, 2017.

[20] A. Hojjati, A. Adhikari, K. Struckmann, E. Chou, T. N. Tho Nguyen, K. Madan, M. S. Winslett, C. A. Gunter, and W. P. King, "Leave your phone at the door: Side channels that reveal factory floor secrets," in *Proceedings of the 2016 ACM SIGSAC Conference on Computer and Communications Security*, 2016, pp. 883–894.

[21] S. R. Chhetri, A. Barua, S. Faezi, F. Regazzoni, A. Canedo, and M. A. Al Faruque, "Tool of spies: Leaking your ip by altering the 3d printer compiler," *IEEE Transactions on Dependable and Secure Computing*, vol. 18, no. 2, pp. 667–678, 2019.

[22] S. B. Moore, W. B. Glisson, and M. Yampolskiy, "Implications of malicious 3d printer firmware," in *Proceedings of the 50th Hawaii International Conference on System Sciences*, 2017.

[23] H. Pearce, K. Yanamandra, N. Gupta, and R. Karri, "Flaw3d: A trojan-based cyber attack on the physical outcomes of additive manufacturing," *IEEE/ASME Transactions on Mechatronics*, 2022.

[24] J. Gatlin, S. Belikovetsky, S. B. Moore, Y. Solewicz, Y. Elovici, and M. Yampolskiy, "Detecting sabotage attacks in additive manufacturing using actuator power signatures," *IEEE Access*, vol. 7, pp. 133 421–133 432, 2019.

[25] S. Belikovetsky, Y. A. Solewicz, M. Yampolskiy, J. Toh, and Y. Elovici, "Digital audio signature for 3d printing integrity," *ieee transactions on information forensics and security*, vol. 14, no. 5, pp. 1127–1141, 2018.

[26] S.-Y. Yu, A. V. Malawade, S. R. Chhetri, and M. A. Al Faruque, "Sabotage attack detection for additive manufacturing systems," *IEEE Access*, vol. 8, pp. 27 218–27 231, 2020.

[27] S. R. Chhetri, A. Canedo, and M. A. Al Faruque, "Kcad: kinetic cyber-attack detection method for cyber-physical additive manufacturing systems," in *2016 IEEE/ACM International Conference on Computer-Aided Design (ICCAD)*. IEEE, 2016, pp. 1–8.

[28] M. Rott and S. A. S. Monroy, "Power-based intrusion detection for additive manufacturing: A deep learning approach," in *International Conference on Industrial IoT Technologies and Applications*. Springer, 2020, pp. 171–189.

[29] C. Bayens, T. Le, L. Garcia, R. Beyah, M. Javanmard, and S. Zonouz, "See no evil, hear no evil, feel no evil, print no evil? malicious fill patterns detection in additive manufacturing," in *26th USENIX Security Symposium (USENIX Security 17)*, 2017, pp. 1181–1198.

[30] M. Wu, Z. Song, and Y. B. Moon, "Detecting cyber-physical attacks in cybermanufacturing systems with machine learning methods," *Journal of intelligent manufacturing*, vol. 30, no. 3, pp. 1111–1123, 2019.

[31] M. Wu, H. Zhou, L. L. Lin, B. Silva, Z. Song, J. Cheung, and Y. Moon, "Detecting attacks in cybermanufacturing systems: Additive manufacturing example," in *MATEC Web of Conferences*, vol. 108. EDP Sciences, 2017, p. 06005.

[32] A. Al Mamun, C. Liu, C. Kan, and W. Tian, "Securing cyber-physical additive manufacturing systems by in-situ process authentication using streamline video analysis," *Journal of Manufacturing Systems*, vol. 62, pp. 429–440, 2022.

[33] ——, "Real-time process authentication for additive manufacturing processes based on in-situ video analysis," *Procedia Manufacturing*, vol. 53, pp. 697–704, 2021.

[34] Z. Shi, A. A. Mamun, C. Kan, W. Tian, and C. Liu, "An lstm-autoencoder based online side channel monitoring approach for cyber-physical attack detection in additive manufacturing," *Journal of Intelligent Manufacturing*, pp. 1–17, 2022.

[35] H. Zhou, C. Liu, W. Tian, and C. Kan, "Echo state network learning for the detection of cyber attacks in additive manufacturing," in *2021 IEEE 17th International Conference on Automation Science and Engineering (CASE)*. IEEE, 2021, pp. 177–182.

[36] Y. Gao, B. Li, W. Wang, W. Xu, C. Zhou, and Z. Jin, "Watching and safeguarding your 3d printer: Online process monitoring against cyber-physical attacks," *Proceedings of the ACM on Interactive, Mobile, Wearable and Ubiquitous Technologies*, vol. 2, no. 3, pp. 1–27, 2018.

[37] M. H. Rais, M. Ahsan, V. Sharma, R. Barua, R. Prins, and I. Ahmed, "Low-magnitude infill structure manipulation attacks on fused filament fabrication 3d printers," in *Critical Infrastructure Protection XVI: 16th IFIP WG 11.10 International Conference, ICCIP 2022*. Springer, 2022, pp. 205–232.

[38] M. H. Rais, Y. Li, and I. Ahmed, "Spatiotemporal g-code modeling for secure fdm-based 3d printing," in *Proceedings of the ACM/IEEE 12th International Conference on Cyber-Physical Systems*, 2021, pp. 177–186.

[39] S. Liang, X. Peng, H. J. Qi, S. Zonouz, and R. Beyah, "A practical side-channel based intrusion detection system for additive manufacturing systems," in *2021 IEEE 41st International Conference on Distributed Computing Systems (ICDCS)*. IEEE, 2021, pp. 1075–1087.

[40] S. E. Zeltmann, N. Gupta, N. G. Tsoutsos, M. Maniatakos, J. Rajendran, and R. Karri, "Manufacturing and security challenges in 3d printing," *Jom*, vol. 68, no. 7, pp. 1872–1881, 2016.

[41] J. Straub, "3d printing cybersecurity: detecting and preventing attacks that seek to weaken a printed object by changing fill level," in *Dimensional optical metrology and inspection for practical applications VI*, vol. 10220. SPIE, 2017, pp. 90–104.

[42] ——, "Identifying positioning-based attacks against 3d printed objects and the 3d printing process," in *Pattern Recognition and Tracking XXVIII*, vol. 10203. SPIE, 2017, pp. 22–34.

[43] ——, "An approach to detecting deliberately introduced defects and micro-defects in 3d printed objects," in *Pattern Recognition and Tracking XXVIII*, vol. 10203. SPIE, 2017, pp. 144–157.

[44] ——, "A combined system for 3D printing cybersecurity," in *Dimensional Optical Metrology and Inspection for Practical Applications VI*, vol. 10220, International Society for Optics and Photonics. SPIE, 2017, p. 102200N.

[45] ——, "Physical security and cyber security issues and human error prevention for 3d printed objects: detecting the use of an incorrect printing material," in *Dimensional Optical Metrology and Inspection for Practical Applications VI*, vol. 10220. SPIE, 2017, pp. 90–105.

[46] M. H. Rais, M. Ahsan, and I. Ahmed, "Fromepp: Digital forensic readiness framework for material extrusion based 3d printing process," 2023.

[47] L. D. Sturm, C. B. Williams, J. A. Camelio, J. White, and R. Parker, "Cyber-physical vulnerabilities in additive manufacturing systems," in *2014 International Solid Freeform Fabrication Symposium*. University of Texas at Austin, 2014.

[48] P. K. Mishra, P. Senthil, S. Adarsh, and M. Anoop, "An investigation to study the combined effect of different infill pattern and infill density on the impact strength of 3d printed polylactic acid parts," *Composites Communications*, vol. 24, p. 100605, 2021.

[49] M. Rismalia, S. Hidajat, I. Permana, B. Hadisujoto, M. Muslimin, and F. Triawan, "Infill pattern and density effects on the tensile properties of 3d printed pla material," in *Journal of Physics: Conference Series*, vol. 1402, no. 4. IOP Publishing, 2019, p. 044041.

[50] M. Tanveer, A. Haleem, M. Suhaib *et al.*, "Effect of variable infill density on mechanical behaviour of 3-d printed pla specimen: an experimental investigation," *SN Applied Sciences*, vol. 1, no. 12, pp. 1–12, 2019.

[51] Ö. Bayraktar, G. Uzun, R. Çakiroğlu, and A. Guldas, "Experimental study on the 3d-printed plastic parts and predicting the mechanical properties using artificial neural networks," *Polymers for Advanced Technologies*, vol. 28, no. 8, pp. 1044–1051, 2017.

[52] M. Kaveh, M. Badrossamay, E. Foroozmehr, and A. H. Etefagh, "Optimization of the printing parameters affecting dimensional accuracy and internal cavity for hips material used in fused deposition modeling processes," *Journal of materials processing technology*, vol. 226, pp. 280–286, 2015.

[53] S. Kumar, V. N. Kannan, and G. Sankaranarayanan, "Parameter optimization of abs-m30i parts produced by fused deposition modeling for minimum surface roughness," *International Journal of Current Engineering and Technology*, vol. 3, pp. 93–97, 2014.

[54] J. Martínez, J. Diéguez, A. Pereira, and J. Pérez, "Modelization of surface roughness in fdm parts," in *AIP Conference Proceedings*, vol. 1431, no. 1. American Institute of Physics, 2012, pp. 849–856.

[55] I. Buj-Corral, A. Domínguez-Fernández, and R. Durán-Lluchà, "Influence of print orientation on surface roughness in fused deposition modeling (fdm) processes," *Materials*, vol. 12, no. 23, p. 3834, 2019.

[56] C. Liu, A. C. C. Law, D. Roberson, and Z. J. Kong, "Image analysis-based closed loop quality control for additive manufacturing with fused filament fabrication," *Journal of Manufacturing Systems*, vol. 51, pp. 75–86, 2019.

[57] M. Spoerk, C. Holzer, and J. Gonzalez-Gutierrez, "Material extrusion-based additive manufacturing of polypropylene: A review on how to improve dimensional inaccuracy and warpage," *Journal of Applied Polymer Science*, vol. 137, no. 12, p. 48545, 2020.

[58] C. Casavola, A. Cazzato, D. Karalekas, V. Moramarco, and G. Pappalettera, "The effect of chamber temperature on residual stresses of fdm parts," in *Residual Stress, Thermomechanics & Infrared Imaging, Hybrid Techniques and Inverse Problems, Volume 7*. Springer, 2019, pp. 87–92.

[59] A. Armillotta, M. Bellotti, and M. Cavallaro, "Warpage of fdm parts: Experimental tests and analytic model," *Robotics and Computer-Integrated Manufacturing*, vol. 50, pp. 140–152, 2018.

[60] B. N. Panda, K. Shankhwar, A. Garg, and Z. Jian, "Performance evaluation of warping characteristic of fused deposition modelling process," *The International Journal of Advanced Manufacturing Technology*, vol. 88, no. 5, pp. 1799–1811, 2017.

[61] D. Pollard, C. Ward, G. Herrmann, and J. Etches, "Filament temperature dynamics in fused deposition modelling and outlook for control," *Procedia Manufacturing*, vol. 11, pp. 536–544, 2017.

[62] S. Costa, F. Duarte, and J. Covas, "Estimation of filament temperature and adhesion development in fused deposition techniques," *Journal of Materials Processing Technology*, vol. 245, pp. 167–179, 2017.

[63] J. E. Seppala and K. D. Migler, "Infrared thermography of welding zones produced by polymer extrusion additive manufacturing," *Additive manufacturing*, vol. 12, pp. 71–76, 2016.

[64] J. E. Seppala, S. H. Han, K. E. Hillgartner, C. S. Davis, and K. B. Migler, "Weld formation during material extrusion additive manufacturing," *Soft matter*, vol. 13, no. 38, pp. 6761–6769, 2017.

[65] C. S. Davis, K. E. Hillgartner, S. H. Han, and J. E. Seppala, "Mechanical strength of welding zones produced by polymer extrusion additive manufacturing," *Additive manufacturing*, vol. 16, pp. 162–166, 2017.

[66] H. Li, Z. Yu, F. Li, Q. Kong, and J. Tang, "Real-time polymer flow state monitoring during fused filament fabrication based on acoustic emission," *Journal of Manufacturing Systems*, vol. 62, pp. 628–635, 2022.

[67] J. Nam, N. Jo, J. S. Kim, and S. W. Lee, "Development of a health monitoring and diagnosis framework for fused deposition modeling process based on a machine learning algorithm," *Proceedings of the Institution of Mechanical Engineers, Part B: Journal of Engineering Manufacture*, vol. 234, no. 1-2, pp. 324–332, 2020.

[68] H. Wu, Z. Yu, and Y. Wang, "A new approach for online monitoring of additive manufacturing based on acoustic emission," in *International Manufacturing Science and Engineering Conference*, vol. 49910. American Society of Mechanical Engineers, 2016, p. V003T08A013.

[69] H. Wu, Y. Wang, and Z. Yu, "In situ monitoring of fdm machine condition via acoustic emission," *The International Journal of Advanced Manufacturing Technology*, vol. 84, no. 5, pp. 1483–1495, 2016.

[70] H. Wu, Z. Yu, and Y. Wang, "Real-time fdm machine condition monitoring and diagnosis based on acoustic emission and hidden semi-markov model," *The International Journal of Advanced Manufacturing Technology*, vol. 90, no. 5, pp. 2027–2036, 2017.

[71] J. Liu, Y. Hu, B. Wu, and Y. Wang, "An improved fault diagnosis approach for fdm process with acoustic emission," *Journal of Manufacturing Processes*, vol. 35, pp. 570–579, 2018.

[72] F. Li, Z. Yu, X. Shen, and H. Zhang, "Status recognition for fused deposition modeling manufactured parts based on acoustic emission," in *E3S Web of Conferences*, vol. 95. EDP Sciences, 2019, p. 01005.

[73] H. Wu, Z. Yu, and Y. Wang, "Experimental study of the process failure diagnosis in additive manufacturing based on acoustic emission," *Measurement*, vol. 136, pp. 445–453, 2019.

[74] F. Li, Z. Yu, Z. Yang, and X. Shen, "Real-time distortion monitoring during fused deposition modeling via acoustic emission," *Structural Health Monitoring*, vol. 19, no. 2, pp. 412–423, 2020.

[75] Y. Lu and Y. Wang, "Machine fault diagnosis of fused filament fabrication process with physics-constrained dictionary learning," *Procedia Manufacturing*, vol. 53, pp. 726–734, 2021.

[76] Z. Yang, L. Jin, Y. Yan, and Y. Mei, "Filament breakage monitoring in fused deposition modeling using acoustic emission technique," *Sensors*, vol. 18, no. 3, p. 749, 2018.

[77] H. Parker, S. Psulkowski, P. Tran, and T. Dickens, "In-situ print characterization and defect monitoring of 3d printing via conductive filament and ohm's law," *Procedia Manufacturing*, vol. 53, pp. 417–426, 2021.

[78] C. Kim, D. Espalin, A. Cuaron, M. A. Perez, E. MacDonald, and R. B. Wicker, "A study to detect a material deposition status in fused deposition modeling technology," in *2015 IEEE International Conference on Advanced Intelligent Mechatronics (AIM)*. IEEE, 2015, pp. 779–783.

[79] Y. Tlegenov, W. F. Lu, and G. S. Hong, "A dynamic model for current-based nozzle condition monitoring in fused deposition modelling," *Progress in Additive Manufacturing*, vol. 4, no. 3, pp. 211–223, 2019.

[80] Y. Lu and Y. Wang, "Monitoring temperature in additive manufacturing with physics-based compressive sensing," *Journal of manufacturing systems*, vol. 48, pp. 60–70, 2018.

[81] ——, "An efficient transient temperature monitoring of fused filament fabrication process with physics-based compressive sensing," *IISE Transactions*, vol. 51, no. 2, pp. 168–180, 2019.

[82] ——, "An improvement of physics based compressive sensing with domain decomposition to monitor temperature in fused filament fabrication process," in *International Manufacturing Science and Engineering Conference*, vol. 58745. American Society of Mechanical Engineers, 2019, p. V001T01A032.

[83] Y. Lu, E. Shevtshenko, and Y. Wang, "Physics-based compressive sensing to enable digital twins of additive manufacturing processes," *Journal of Computing and Information Science in Engineering*, vol. 21, no. 3, 2021.

[84] E. Ferraris, J. Zhang, and B. Van Hooreweder, "Thermography based in-process monitoring of fused filament fabrication of polymeric parts," *CIRP Annals*, vol. 68, no. 1, pp. 213–216, 2019.

[85] E. Malekipour, S. Attoye, and H. El-Mounayri, "Investigation of layer based thermal behavior in fused deposition modeling process by infrared thermography," *Procedia Manufacturing*, vol. 26, pp. 1014–1022, 2018.

[86] H. Prajapati, D. Ravoori, and A. Jain, "Measurement and modeling of filament temperature distribution in the standoff gap between nozzle and bed in polymer-based additive manufacturing," *Additive Manufacturing*, vol. 24, pp. 224–231, 2018.

[87] J. Li, R. Jin, and Z. Y. Hang, "Integration of physically-based and data-driven approaches for thermal field prediction in additive manufacturing," *Materials & Design*, vol. 139, pp. 473–485, 2018.

[88] F. Caltanissetta, G. Dreifus, A. J. Hart, and B. M. Colosimo, "In-situ monitoring of material extrusion processes via thermal videoimaging with application to big area additive manufacturing (baam)," *Additive Manufacturing*, vol. 58, p. 102995, 2022.

[89] K. He, H. Wang, and H. Hu, "Approach to online defect monitoring in fused deposition modeling based on the variation of the temperature field," *Complexity*, vol. 2018, 2018.

[90] H. Hu, K. He, T. Zhong, and Y. Hong, "Fault diagnosis of fdm process based on support vector machine (svm)," *Rapid Prototyping Journal*, 2019.

[91] Y. Banadaki, N. Razaviarab, H. Fekrmandi, and S. Sharifi, "Toward enabling a reliable quality monitoring system for additive manufacturing process using deep convolutional neural networks," *arXiv preprint arXiv:2003.08749*, 2020.

[92] Z. Jin, Z. Zhang, and G. X. Gu, "Autonomous in-situ correction of fused deposition modeling printers using computer vision and deep learning," *Manufacturing Letters*, vol. 22, pp. 11–15, 2019.

[93] Z. Zhang, I. Fidan, and M. Allen, "Detection of material extrusion in-process failures via deep learning," *Inventions*, vol. 5, no. 3, p. 25, 2020.

[94] F. Baumann and D. Roller, "Vision based error detection for 3d printing processes," in *MATEC web of conferences*, vol. 59. EDP Sciences, 2016, p. 06003.

[95] A. Petsiuk and J. M. Pearce, "Towards smart monitored am: Open source in-situ layer-wise 3d printing image anomaly detection using histograms of oriented gradients and a physics-based rendering engine," *Additive Manufacturing*, vol. 52, p. 102690, 2022.

[96] A. Ceruti, A. Liverani, and T. Bombardi, "Augmented vision and interactive monitoring in 3d printing process," *International Journal on Interactive Design and Manufacturing (IJIDeM)*, vol. 11, no. 2, pp. 385–395, 2017.

[97] A. Malik, H. Lhachemi, J. Ploennigs, A. Ba, and R. Shorten, "An application of 3d model reconstruction and augmented reality for real-time monitoring of additive manufacturing," *Procedia Cirp*, vol. 81, pp. 346–351, 2019.

[98] J. Straub, "Initial work on the characterization of additive manufacturing (3d printing) using software image analysis," *Machines*, vol. 3, no. 2, pp. 55–71, 2015.

[99] ——, "Characterization of 3d printing output using an optical sensing system," in *Dimensional Optical Metrology and Inspection for Practical Applications IV*, vol. 9489. SPIE, 2015, pp. 51–59.

[100] ——, "Alignment issues, correlation techniques and their assessment for a visible light imaging-based 3d printer quality control system," in *Image Sensing Technologies: Materials, Devices, Systems, and Applications III*, vol. 9854. SPIE, 2016, pp. 158–165.

[101] S. Nuchitprasitchai, M. Roggemann, and J. M. Pearce, "Factors effecting real-time optical monitoring of fused filament 3d printing," *Progress in Additive Manufacturing*, vol. 2, no. 3, pp. 133–149, 2017.

[102] S. Nuchitprasitchai, M. C. Roggemann, and J. M. Pearce, "Three hundred and sixty degree real-time monitoring of 3-d printing using computer analysis of two camera views," *Journal of Manufacturing and Materials Processing*, vol. 1, no. 1, p. 2, 2017.

[103] C. Kopsacheilis, P. Charalampous, I. Kostavelis, and D. Tzovaras, "In situ visual quality control in 3d printing." in *VISIGRAPP (3: IVAPP)*, 2020, pp. 317–324.

[104] P. Charalampous, I. Kostavelis, C. Kopsacheilis, and D. Tzovaras, "Vision-based real-time monitoring of extrusion additive manufacturing processes for automatic manufacturing error detection," *The International Journal of Advanced Manufacturing Technology*, vol. 115, no. 11, pp. 3859–3872, 2021.

[105] R. Li, M. Jin, and V. C. Paquit, "Geometrical defect detection for additive manufacturing with machine learning models," *Materials & Design*, vol. 206, p. 109726, 2021.

[106] K. He, Q. Zhang, and Y. Hong, "Profile monitoring based quality control method for fused deposition modeling process," *Journal of Intelligent Manufacturing*, vol. 30, no. 2, pp. 947–958, 2019.

[107] W. Yi, H. Ketai, Z. Xiaomin, and D. Wenying, "Machine vision based statistical process control in fused deposition modeling," in *2017 12th IEEE Conference on Industrial Electronics and Applications (ICIEA)*. IEEE, 2017, pp. 936–941.

[108] W. Yi, H. Ketai, H. Huaqing, and Z. Xue, "Process monitoring of fused deposition modeling through profile control," in *2018 IEEE International Conference on Cyborg and Bionic Systems (CBS)*. IEEE, 2018, pp. 346–350.

[109] J. Fastowicz and K. Okarma, "Texture based quality assessment of 3d prints for different lighting conditions," in *International Conference on Computer Vision and Graphics*. Springer, 2016, pp. 17–28.

[110] K. Okarma, J. Fastowicz, and M. Tecław, "Application of structural similarity based metrics for quality assessment of 3d prints," in *International Conference on Computer Vision and Graphics*. Springer, 2016, pp. 244–252.

[111] K. Okarma and J. Fastowicz, "No-reference quality assessment of 3d prints based on the glcm analysis," in *2016 21st International Conference on Methods and Models in Automation and Robotics (MMAR)*. IEEE, 2016, pp. 788–793.

[112] ——, "Quality assessment of 3d prints based on feature similarity metrics," in *International Conference on Image Processing and Communications*. Springer, 2016, pp. 104–111.

[113] J. Fastowicz, D. Bak, P. Mazurek, and K. Okarma, "Quality assessment of 3d printed surfaces in fourier domain," in *International Conference on Image Processing and Communications*. Springer, 2017, pp. 75–81.

[114] ——, "Estimation of geometrical deformations of 3d prints using local cross-correlation and monte carlo sampling," in *International Conference on Image Processing and Communications*. Springer, 2017, pp. 67–74.

[115] P. Lech, J. Fastowicz, and K. Okarma, "Quality evaluation of 3d printed surfaces based on hog features," in *International Conference on Computer Vision and Graphics*. Springer, 2018, pp. 199–208.

[116] J. law Fastowicz and K. Okarma, "Quality assessment of photographed 3 d printed flat surfaces using hough transform and histogram equalization," *J. Univers. Comput. Sci*, vol. 25, no. 6, pp. 701–717, 2019.

[117] J. Fastowicz and K. Okarma, "Automatic colour independent quality evaluation of 3d printed flat surfaces based on clahe and hough transform," in *International Conference on Image Processing and Communications*. Springer, 2018, pp. 123–131.

[118] K. Okarma and J. Fastowicz, "Color independent quality assessment of 3d printed surfaces based on image entropy," in *International Conference on Computer Recognition Systems*. Springer, 2017, pp. 308–315.

[119] ——, "Improved quality assessment of colour surfaces for additive manufacturing based on image entropy," *Pattern Analysis and Applications*, vol. 23, no. 3, pp. 1035–1047, 2020.

[120] J. Fastowicz and K. Okarma, "Entropy based surface quality assessment of 3d prints," in *Computer Science On-line Conference*. Springer, 2017, pp. 404–413.

[121] J. Fastowicz, M. Grudziński, M. Tecław, and K. Okarma, "Objective 3d printed surface quality assessment based on entropy of depth maps," *Entropy*, vol. 21, no. 1, p. 97, 2019.

[122] K. Okarma, J. Fastowicz, P. Lech, and V. Lukin, "Quality assessment of 3d printed surfaces using combined metrics based on mutual structural similarity approach correlated with subjective aesthetic evaluation," *Applied Sciences*, vol. 10, no. 18, p. 6248, 2020.

[123] K. Okarma and J. Fastowicz, "Adaptation of full-reference image quality assessment methods for automatic visual evaluation of the surface quality of 3d prints," *Elektronika ir Elektrotechnika*, vol. 25, no. 5, pp. 57–62, 2019.

[124] ——, "Computer vision methods for non-destructive quality assessment in additive manufacturing," in *International Conference on Computer Recognition Systems*. Springer, 2019, pp. 11–20.

[125] J. Fastowicz, P. Lech, and K. Okarma, "Combined metrics for quality assessment of 3d printed surfaces for aesthetic purposes: Towards higher accordance with subjective evaluations," in *International Conference on Computational Science*. Springer, 2020, pp. 326–339.

[126] T. Huang, S. Wang, S. Yang, and W. Dai, "Statistical process monitoring in a specified period for the image data of fused deposition modeling parts with consistent layers," *Journal of Intelligent Manufacturing*, vol. 32, no. 8, pp. 2181–2196, 2021.

[127] D. Blanco, P. Fernandez, A. Noriega, B. J. Alvarez, and G. Valiño, "Layer contour verification in additive manufacturing by means of commercial flatbed scanners," *Sensors*, vol. 20, no. 1, p. 1, 2019.

[128] J. Li, H. Xie, and K. Ma, "In-situ monitoring of the deformation during fused deposition modeling process using cgs method," *Polymer Testing*, vol. 76, pp. 166–172, 2019.

[129] A. Saluja, J. Xie, and K. Fayazbakhsh, "A closed-loop in-process warping detection system for fused filament fabrication using convolutional neural networks," *Journal of Manufacturing Processes*, vol. 58, pp. 407–415, 2020.

[130] G. P. Greeff and M. Schilling, "Closed loop control of slippage during filament transport in molten material extrusion," *Additive Manufacturing*, vol. 14, pp. 31–38, 2017.

[131] E. Soriano Heras, F. Blaya Haro, J. M. De Agustín del Burgo, M. Islán Marcos, and R. D'Amato, "Filament advance detection sensor for fused deposition modelling 3d printers," *Sensors*, vol. 18, no. 5, p. 1495, 2018.

[132] M. Faes, W. Abbeloos, F. Vogeler, H. Valkenaers, K. Coppens, T. Goedemé, and E. Ferraris, "Process monitoring of extrusion based 3d printing via laser scanning," *arXiv preprint arXiv:1612.02219*, 2016.

[133] L. Li, R. McGuan, P. Kavehpour, and R. Candler, "Precision enhancement of 3d printing via in situ metrology," in *2018 International Solid Freeform Fabrication Symposium*. University of Texas at Austin, 2018.

[134] L. Li, R. McGuan, R. Isaac, P. Kavehpour, and R. Candler, "Improving precision of material extrusion 3d printing by in-situ monitoring & predicting 3d geometric deviation using conditional adversarial networks," *Additive Manufacturing*, vol. 38, p. 101695, 2021.

[135] W. Lin, H. Shen, J. Fu, and S. Wu, "Online quality monitoring in material extrusion additive manufacturing processes based on laser scanning technology," *Precision Engineering*, vol. 60, pp. 76–84, 2019.

[136] M. Moretti and N. Senin, "In-process monitoring of part warpage in fused filament fabrication through the analysis of the repulsive force acting on the extruder," *Additive Manufacturing*, vol. 49, p. 102505, 2022.

[137] T. J. Coogan and D. O. Kazmer, "Prediction of interlayer strength in material extrusion additive manufacturing," *Additive Manufacturing*, vol. 35, p. 101368, 2020.

[138] ——, "In-line rheological monitoring of fused deposition modeling," *Journal of Rheology*, vol. 63, no. 1, pp. 141–155, 2019.

[139] D. A. Anderegg, H. A. Bryant, D. C. Ruffin, S. M. Skrip Jr, J. J. Fallon, E. L. Gilmer, and M. J. Bortner, "In-situ monitoring of polymer flow temperature and pressure in extrusion based additive manufacturing," *Additive Manufacturing*, vol. 26, pp. 76–83, 2019.

[140] F. Peng, B. D. Vogt, and M. Cakmak, "Complex flow and temperature history during melt extrusion in material extrusion additive manufacturing," *Additive Manufacturing*, vol. 22, pp. 197–206, 2018.

[141] S. Bukkapatnam and B. Clark, "Dynamic Modeling and Monitoring of Contour Crafting—An Extrusion-Based Layered Manufacturing Process," *Journal of Manufacturing Science and Engineering*, vol. 129, no. 1, pp. 135–142, 08 2006.

[142] Y. Tlegenov, G. S. Hong, and W. F. Lu, "Nozzle condition monitoring in 3d printing," *Robotics and Computer-Integrated Manufacturing*, vol. 54, pp. 45–55, 2018.

[143] P. K. Rao, J. P. Liu, D. Roberson, Z. J. Kong, and C. Williams, "Online real-time quality monitoring in additive manufacturing processes using heterogeneous sensors," *Journal of Manufacturing Science and Engineering*, vol. 137, no. 6, 2015.

[144] K. Bastani, P. K. Rao, and Z. Kong, "An online sparse estimation-based classification approach for real-time monitoring in advanced manufacturing processes from heterogeneous sensor data," *IIE Transactions*, vol. 48, no. 7, pp. 579–598, 2016.

[145] J. S. Kim, C. S. Lee, S.-M. Kim, and S. W. Lee, "Development of data-driven in-situ monitoring and diagnosis system of fused deposition modeling (fdm) process based on support vector machine algorithm," *International Journal of Precision Engineering and Manufacturing-Green Technology*, vol. 5, no. 4, pp. 479–486, 2018.

[146] S. Hurd, C. Camp, and J. White, "Quality assurance in additive manufacturing through mobile computing," in *International Conference on Mobile Computing, Applications, and Services*. Springer, 2015, pp. 203–220.

[147] U. Delli and S. Chang, "Automated process monitoring in 3d printing using supervised machine learning," *Procedia Manufacturing*, vol. 26, pp. 865–870, 2018.

[148] B. Macq, P. R. Alface, and M. Montanola, "Applicability of watermarking for intellectual property rights protection in a 3d printing scenario," in *Proceedings of the 20th International Conference on 3D Web Technology*, 2015, pp. 89–95.
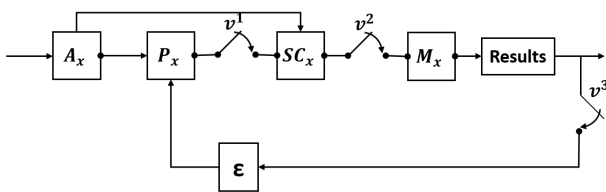
Appendix

Figure 5. Generic SC framework for monitoring process anomalies

Generic side channel framework for anomaly detection. A generic SC framework for detecting and monitoring printing process anomalies is presented in Figure. 5. In here $'A_x'$ are the printing anomalies, $'P_x'$ are printing parameters, $'SC_x'$ represent side channels, and $'Mx'$ are the methodologies used to interpret SC information for the detection and monitoring of process anomalies. v^x are the decision variables to choose between different available SCs and methodologies, details of which are as follows;

- v^1 is the decision variable to choose among different available SCs and is dependent on multiple factors such as
    - Sensitivity defines the ability of SC to detect subtle changes.
    - Specificity defines the ability to differentiate amongst different process anomalies.
    - Printing parameter states which process variables are to be monitored using SC.
    - Non-intrusiveness states the SC's ability to take measurements without changing/affecting the printing process.
    - Real-time states the performance ability for rapid detection of process anomalies.
    - Interpretability defines how readily usable the SC information is.
    - Cost effectiveness is another parameter to be considered while selecting sensing equipment.

- v^2 decides which methodology to apply to the collected SC information and is based on the following factors
    - Performance states the accuracy of the methodology for detecting a particular process anomaly using specific SC information.
    - Scalability defines the ability of the methodology to incorporate new process information without affecting system stability.
    - Generalization states the results should be inclusive for a wide range of printing environments.

- v^3 engages the closed-loop control of the monitoring process. The loop could be used to either stop the printing process or adjust the printing parameters.
- ϵ is the error value that is calculated from the monitoring results and is adjusted in the printing parameters.

The proposed generic framework provides the user with a tool to consider which variables while considering a monitoring system. The following example illustrates the use of the proposed framework. Let's assume a user is interested in finding anomalies of type 'void' (A_{vd}) in their printing environment. The parameters associated with this anomaly are $P_{if}, P_{nt}, P_{ef}, P_{ns}, P_{ax}$ as shown in Figure 4. To monitor these parameters, the user needs to select a suitable side channel. As per the literature, the best accuracy obtained for these parameters is through the use of SC_H (see Table 6) and the methodology $M3$ (see Table 8). Owing to other factors (such as intrusiveness), a user may opt for other SCs as well.